Storage Ring Design
as a
Synchrotron Light Source

Helmut Wiedemann
Stanford University

School on Synchrotron Radiation
April 19 - 24, 2004
Abdus Salam Int. Center for Theoretical Physics, ICTP
Trieste, Italy

Abstract

In these lecture notes we address specific design features for a synchrotron radiation source. Starting with fundamental aspects of beam dynamics we develop an overview of the physics of electron beam storage rings and derive scaling laws for the beam emittance which ultimately determines the photon beam brightness.

1 Storage Ring System

A beam of charged particles can emit *synchrotron radiation* whenever it is deflected by a magnetic or electric field. The intensity and spectrum of the radiation depends greatly on the mass of the charged particle. For this reason only electron or positron beams are considered as potential synchrotron radiation sources. Furthermore, the intensity and spectrum of synchrotron radiation is greatly enhanced and other photon beam characteristics are significantly improved if highly relativistic particles are considered. We concentrate therefore on accelerator systems which can produce highly relativistic electron beams.

The energy of an electron is measured in units of an "electron Volt". This is equal to the kinetic energy gained by an electron while being accelerated in the field between two electrodes with a potential difference of 1 Volt. Electrons become relativistic if their kinetic energy exceeds that of the restmass or about 511000 eV. Most synchrotron radiation sources are based on electron beams with kinetic energies of several hundred million electron volts and higher. We use for such high energies the units MeV (10^6 eV) or GeV(10^9) eV. The photon energy of synchrotron radiation is also measured in eV. Photon energies of general interest reach up to about 20 keV, where 1keV=1000 eV. For scaling it is useful to remember that a x-ray photon wavelength of 1Å is equivalent to an energy of 12398 eV or 12.4 keV.

In our brief overview on accelerator physics we consider only magnetic fields for electron beam guidance since technically feasible magnetic fields are much more effective than realistic electric fields (1 Tesla of magnetic field corresponds to $3 \cdot 10^8$ Volt/m of electric field). For application and research one would like to have a continuous emission of photons which can be accomplished in an electron *storage ring*.

A storage ring is a circular accelerator which is widely used as a synchrotron radiation source. After injection, electrons circulate in this ring for several hours at constant energy serving as the source of continuous synchrotron radiation. A storage ring is therefore not a true accelerator although a beam can be accelerated very slowly if required (e.g. if the injection energy is lower than the operating energy). While the electrons circulate in the storage ring they emit electromagnetic radiation wherever they pass through magnetic field. This radiation can be extracted from the ring through long pipes, called *photon beam lines* leading to experimental stations and be used for basic and applied science.

The intensity of synchrotron radiation is proportional to the number of electrons circulating in the storage ring. We define a circulating beam current by

$$I_{\mathrm{b}} = eN_{\mathrm{e}}f_{\mathrm{rev}} \tag{1}$$

where N_{e} is the total number of electrons circulating in the storage ring and f_{rev} is the revolution time.

The storage ring operating at energies above several hundred MeV is enclosed in a concrete tunnel or behind a concrete shielding wall to shield people from ionizing radiation. The photon beam is guided out of this radiation environment through small holes in the shielding wall to the experimental stations.

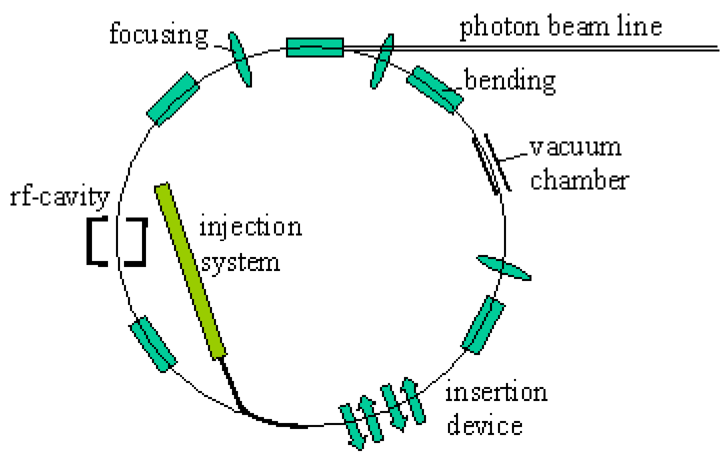

Figure 1: Main Storage Ring Components

To establish and sustain an electron beam in a storage ring, many technical components are required. The nature and functioning of the major ones will be discussed in more detail.

1.1 Component layout

Every circular accelerator is composed of technical components, like magnets, ultra-high vacuum system, rf-system, injector system, beam monitoring, control system etc. Basically, all main components are installed along a closed loop defining the *orbit* along which the electrons travel. In the schematic Fig. 1, the principle layout of the main components is displayed.

1.1.1 Function of components

In this section we give brief descriptions of the functions each of the main storage ring components plays.

- **Magnets**
  - *bending magnets* are used to deflect the electron beam. Placing bending magnets in a well ordered arrangement such as to form a closed ring forces the beam to follow a closed path around the circular accelerator. The location of bending magnets defines the geometry of the storage ring. Although we call this a circular accelerator the shape

is actually not circular. A series of arc sections (bending magnets) is interrupted by straight sections to make space for other components. Bending magnets also serve as sources of synchrotron radiation.

  - *quadrupole magnets* are placed in straight sections between bending magnets to prevent by focusing particles from deviating too much from the orbital path, *ideal orbit*. As such, quadrupoles act much like glass lenses in light optics. We borrow many terms and techniques from light optics since the functions are very similar.
  - *sextupole magnets* are used to correct for chromatic aberrations caused by focusing errors on particles with different energies.

- **Vacuum chamber**
  - The electron beam must be enclosed in a vacuum chamber where the air pressure is reduced to some 10^{-9} Torr or lower to prevent particle losses due to scattering on residual gas atoms. Electrons, once injected into a storage ring are expected to circulate for many hours and produce synchrotron radiation with a minimum rate of loss. This low pressure is achieved by placing many vacuum pumps along the circular path. Due to gas desorption by radiation hitting the vacuum chamber surface continuous pumping is required.

- **Rf-system**
  - Electrons are expected to circulate for many hours at constant energy in a storage ring to produce synchrotron radiation. Although the particle energy is kept constant, energy loss into synchrotron radiation occurs and must be compensated by equivalent acceleration. Special accelerating cavities are installed along the ring generating an accelerating electric field in synchronism with the arrival of electrons. The acceleration exactly compensates for the energy loss to radiation. The electric fields oscillate at frequencies of the order of 500 MHz and proper acceleration occurs only when electrons pass through the cavity at a specific time which is the reason for the bunched character of the circulating electron beam. The circulating beam is composed of one or more clumps, *bunches*, of electrons where the distance between bunches is any integer multiple of the rf-wavelength. For the same reason, the circumference also must be an integer multiple of the rf-wavelength.

- **Beam Controls**
  - A number of beam controls are included in the design of a storage ring. Beam monitors are used to measure the circulating beam current, beam lifetime and transverse beam position. Due to field and alignment errors of main magnets the particle beam follows a distorted closed loop. These distortions must be corrected as much as

possible by *steering magnet*. Generally, a storage ring is controlled by a computer setting and recording component parameters as well as monitoring the beam current and safety equipment.

- **Injection System**
  - Electrons are generated in an injector system consisting of an *electron source*, a low energy accelerator (mostly a *linear accelerator* and a *booster synchrotron* to accelerate the electrons from the low linac energy to the operating energy of the storage ring. After acceleration in the booster the electrons are transferred to the storage ring. To reach high beam intensities in the storage ring many booster pulses are injected.
- **Insertion devices**

  Synchrotron radiation emitted from bending magnets do not always meet all requirements of the users. In order to provide the desired radiation, photon energy, broad band, narrow band etc. insertion devices are placed in magnetfree sections along the orbit. In order not to perturb the ring geometry, such magnets are composed of more than one pole with opposing polarities such that the total beam deflection in the insertion device is zero.
  - *Wiggler* magnets are used to produce high intensity broad band radiation, up to photon energies greatly exceeding that available from the bending magnets. In addition, a wiggler is composed of many poles thus increasing the total photon flux by a factor equal to the number of wiggler poles.
  - *Wavelength Shifters* are generally 3-pole wiggler magnets with a super high field in the central pole to reach hard x-rays in low energy storage rings.
  - *Undulator Magnets* are essentially just weak field wiggler magnets and produce high brightness, quasi monochromatic radiation
  - Other specially designed magnets may produce circularly polarized radiation

2 Beam Guidance and Focusing

Bending and focusing of high energy, relativistic particles is effected by the Lorentz force which is in cgs units (we use formulas written in cgs-system, but switch to MKS units whenever practical formulas are given):

$$\mathbf{F} = e\mathbf{E} + \frac{e}{c}[\mathbf{v} \times \mathbf{B}] \tag{2}$$

One Tesla of magnetic field exerts the same force on a relativistic electron as $3.0 \cdot 10^6$ Volt/cm of electrical field! A magnetic field of 1 Tesla is rather easy

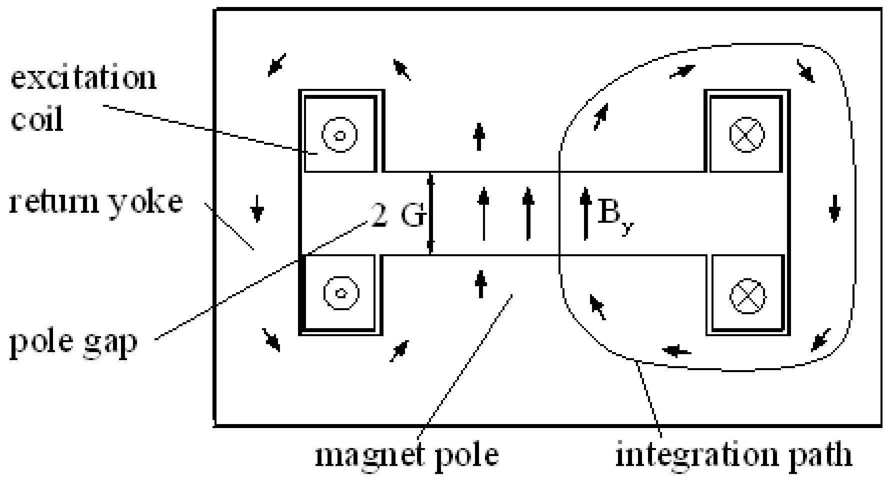

Figure 2: Bending Magnet Cross Section

to produce while the corresponding electric field is beyond technical feasibility. For the manipulation of relativistic particles we use therefore magnetic fields.

2.1 Bending Magnets

Charged particle beams are deflected in *bending magnets.* A transverse magnetic field being constant and homogeneous in space at least in the vicinity of the particle beam, is the lowest order field in beam guidance or beam transport systems. Such a field is called a *dipole field* and can be generated, for example, in an electromagnetic bending magnet with a cross section as shown schematically in Fig. 2

The magnetic field $\mathbf{B}$ is generated by an electrical current I in current carrying coils surrounding magnet poles. A ferromagnetic return yoke surrounds the excitation coils providing an efficient return path for the magnetic flux. The magnetic field is determined by one of Maxwell's equations

$$\nabla \times \frac{\mathbf{B}}{\mu_\mathrm{r}} = \frac{4\pi}{c}\,\mathbf{j}\,, \tag{3}$$

where μ_r is the relative permeability of the ferromagnetic material and $\mathbf{j}$ is the current density in the coils. We integrate (3) over an area enclosed by the integration path shown in Fig. 2 and apply Stoke's theorem to get

$$\int \nabla \times \frac{\mathbf{B}}{\mu_\mathrm{r}} \mathrm{d}A = \oint \frac{\mathbf{B}}{\mu_\mathrm{r}} \mathrm{d}\mathbf{s} = \frac{4\pi}{c} \int \mathbf{j}\mathrm{d}A\,, \tag{4}$$

The integration on the r.h.s. is just the total current in the excitation coils $I_\mathrm{tot} = \int \mathbf{j}\mathrm{d}A$. The l.h.s. must be evaluated along the integration path around the excitation coil. We choose an integration path which is convenient for analytical evaluation. Starting in the middle of the lower magnet pole across the gap we know from symmetry that the magnetic field has only a component B_y which is actually the desired field strength and $\mu_\mathrm{r} = 1$. Within the iron the contribution to the integral vanishes since we assume no saturation effects and set $\mu = \infty$. The integral becomes therefore

$$2\,G\,B_y \;=\; \frac{4\pi}{c}\,2I_\mathrm{tot}\,, \tag{5}$$

where I_tot is the total current through one coil. Solving (5) for the total excitation current in each coil we get in more practical units

$$I_\mathrm{tot}\,(\mathrm{Amp}) \;=\; \frac{10^4}{0.4\pi}\,B_y[\mathrm{T}]\,G[\mathrm{cm}]\,. \tag{6}$$

The total field *excitation current* in the magnet coils is proportional to the desired magnetic field and proportional to the total gap between the magnet poles.

As a practical example, we consider a magnetic field of 1 Tesla in a dipole magnet with a gap of 10 cm. From (6) we find a total electrical current of about 40,000 A is required in each of two excitation coils to generate this field. Since the coil in general is composed of many turns, the actual electrical current is usually much smaller by a factor equal to the number of turns and the total coil current I_tot, therefore, is often measured in units of *Ampere turns*. For example two coils each composed of 40 windings with sufficient cross section to carry an electrical current of 1000 A would provide the total required current of 40,000 A turns each to produce a magnetic field of 1Tesla..

Beam deflection in magnetic field is derived from the equilibrium of centrifugal force and Lorentz force:

$$\frac{\gamma m v^2}{\rho} \;=\; \frac{e}{c}\,vB \tag{7}$$

where we assumed that the direction of the particle velocity $\mathbf{v}$ is orthogonal to the magnetic field: $\mathbf{v}\perp\mathbf{B}$. A pure dipole field deflects a charged particle beam onto a circular path with a bending radius ρ given by

$$\frac{1}{\rho} \;=\; \frac{eB}{\beta E} \tag{8}$$

or in practical units:

$$\frac{1}{\rho}(m^{-1}) \;=\; 0.3\,\frac{B(\mathrm{T})}{cp\,(\mathrm{GeV})} \tag{9}$$

where $\beta = v/c$ and E is the particle energy.
Example: For a field of $B = 1$ Tesla and a particle energy of $E = 1.5$ GeV, the curvature is $1/\rho = 0.2\,\mathrm{m}^{-1}$ or $\rho = 5.0$ m.

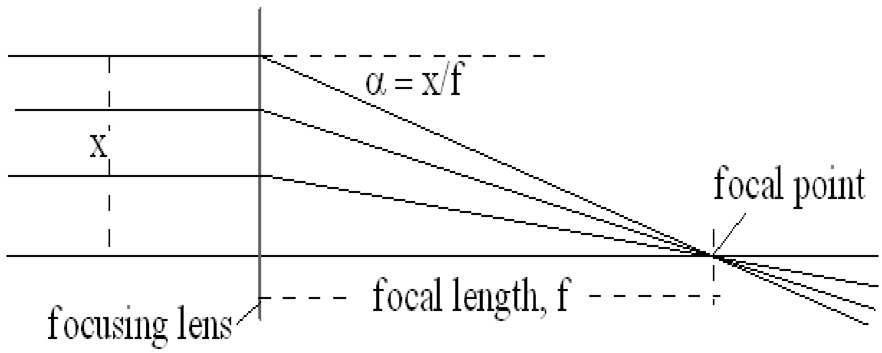

Figure 3: Principle of Focusing

A magnet of length ℓ_b deflects a particle beam by the angle

$$\psi = \ell_\mathrm{b}/\rho\,. \tag{10}$$

Distributing a set of magnets bending the electron beam by appropriate deflection angles along a closed loop establishes the geometric shape of the storage ring.

2.2 Beam Focusing

A ring consisting only of bending magnets would not work since any particle beam has the tendency to spread out. Like a light beam we require focusing elements to confine the particle beam to the vicinity of the orbit defined by the location of the bending magnets.

2.2.1 Principle of Focusing

We borrow much from light optics to describe the focusing of particle beams. To learn how to focus charged particles we recall the principle of focusing in light optic (Fig. 3). The deflection of a light ray parallel to the optical axis by a focusing lens is proportional to the distance of the ray from the optical axis. The distance from the lens where all parallel rays are focused to a pint, the *focal point*, is called the *focal length*.

Applying this to the focusing of particle beams we note from the discussion on bending magnets that the deflection angle is proportional to the length of the magnet and is given by

$$\alpha = \frac{l}{\rho} = \frac{eBl}{cp} \propto x \tag{11}$$

Instead of using a pure dipole field we consider now a field expressed by $B = B_o + gx$ which gives two contributions to the deflection, one is a constant deflection due to the field B_o and the other is an $x$depended deflection

$$\alpha = \frac{egl}{cp}\, x = kl\, x \tag{12}$$

The $x$depended field component gx can be created by a *quadrupole magnet* which therefore functions as the focusing element for charged particle beams. The quantity k is defined as the *quadrupole strength*:

$$k(\mathrm{m}^{-2}) = 0.3\, \frac{g(\mathrm{T/m})}{cp\,(\mathrm{GeV})} \tag{13}$$

and the focal length of the quadrupole is : $1/f = k\ell_q$ where ℓ_q is the length of the quadrupole.

Example: For a focal length of $f = 5$ m and a quadrupole length of $l = 0.2$ m the quadrupole strength and field gradient are: $k = 1.0$ m or $g = 0.5$ kG/cm at a particle energy of 1.5 GeV.

2.2.2 Quadrupol Magnet

How do we produce the desired field gradient or a field: $B_y = gx$ in a quadrupole magnet? Static magnetic field can be derived from a magnetic potential. The field $B_y = gx$ can be derived from the potential $V = -gxy$ by simple differentiation giving the field components

$$B_y = \frac{\partial V}{\partial y} = gx\,, \qquad \text{and} \qquad B_x = \frac{\partial V}{\partial x} = gy\,. \tag{14}$$

Because *ferromagnetic surfaces* are equipotential surfaces (just like metallic surfaces are equipotentials for electric fields) we use magnetic poles shaped in the form of a hyperbola (Fig. 4) given by

$$x \cdot y = \pm\tfrac{1}{2}\, R^2 \tag{15}$$

where R is the aperture radius between the four hyperbolas. A quadrupole is made of four hyperbolic poles with alternating magnetization producing the desired focusing field gradient.

Each of the four pole is excited by electrically powered coils wound around it. Although quadrupoles function as focusing elements just like glass lenses function as focusing elements in light optics there is a fundamental difference. Quadrupoles focus in one plane but defocus in the other depending on the sign of the excitation current, yet the particle beam requires focusing in both planes. To solve this problem we again borrow from light optics the characteristics of focusing in a lens doublet. The focal length of two lenses is $1/f^* = 1/f_1 + 1/f_2 - d/f_1 f_2$ where d is the distance between lenses. If we choose, for example, $f_1 = -f_2 = f$ we get $1/f^* = d\,/\,f^{\,2} > 0$ which is focusing in both planes. By using combinations of focusing and defocusing quadrupoles one can create overall focusing systems. The quadrupoles in a storage ring are therefore polarized

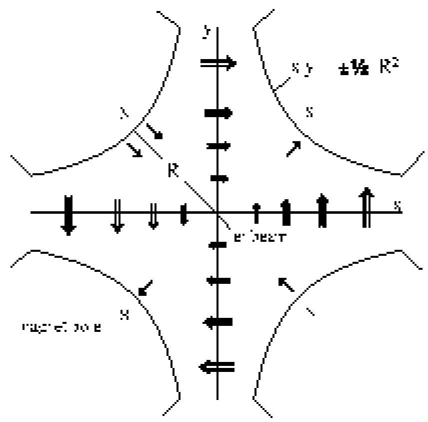

Figure 4: Cross section of a quadrupole magnet, schematic

alternately as focusing or defocusing quadrupoles. It is common in this regard to consider a quadrupole to be focusing if it focuses a particle beam in the horizontal plane. Tacitly, we know that this same quadrupole is defocusing in the vertical plane.

2.3 Single Particle Dynamics

Bending magnets and quadrupoles are the main components to guide and focus a charged particle beam. Furthermore, sextupole magnets are used to correct chromatic aberration introduced by quadrupole focusing. In the following discussion we will formulate mathematical equations to describe the path of individual particles along a beam transport line.

2.3.1 Equation of Motion

The equation of motion in the presence of dipole (B_o), quadrupole (g) and sextupole (g') fields can be derived from the general expression for the curvature $1/\rho$ for paraxial beams ($x' \ll 1$). Here, we define the curvature very general to include all fields (dipole, quadrupole, sextupole...) although in any one magnet only one field type is present. There are exceptions to this separation of fields in some special cases. Specifically, in some new synchrotron light sources we find a combination of a dipole and gradient field in the same bending magnet.

$$\frac{1}{\rho} \approx x'' = \frac{eB}{cp} \tag{16}$$

where

$$\begin{aligned}
B &= B_o + gx + \tfrac{1}{2}\, g'\, x^2 + \ldots \qquad\qquad \text{or} \\
\tfrac{eB}{cp} &= \tfrac{1}{\rho_o} + kx + \tfrac{1}{2}\, mx^2 + \ldots
\end{aligned} \tag{17}$$

With these expansions we get finally the equation of motion

$$\begin{array}{rrl}
x'' = & -kx & \text{focusing term} \\
& +\frac{1}{\rho_o}\delta & \text{dispersion} \\
& +kx\delta & \text{chromatic aberration} \\
& -\frac{1}{2}mx^2 & \text{chromatic and geometric aberration} \\
& \mathcal{O}(3) & \text{higher order terms}
\end{array} \tag{18}$$

Each term in the equation of motion makes its specific (sometimes unwanted) contribution to beam dynamics. Deflection of the beam in a bending magnet depends on the particle energy. Particles with a slightly different energy are deflected differently and this difference cannot be neglected. The same is true for focusing in the form of the chromatic aberration term. Finally we must correct one of the most serious chromatic effect by the installation of sextupole magnets. Unfortunately, such sextupole magnets introduce nonlinear terms into the dynamics causing significant stability problems for particles at large amplitudes.

A similar equation exists for the vertical plane keeping in mind that the magnet parameters must change signs ($k \rightarrow -k$), etc. In the approximation of *linear beam optics* we keep only linear terms and get the differential equation of motion

$$x'' + k(s)x = \frac{1}{\rho_o}\,\delta \tag{19}$$

This equation is similar to that of a perturbed harmonic oscillator although in this case we have a $s$depended restoring force. The solution of this equation is composed of the solution of the homogeneous differential equation and a particular solution of the inhomogeneous differential equation. The physical significance of both solutions is the following. Solutions from the homogeneous equation represent oscillations about an *equilibrium orbit*. Such oscillations are called *betatron oscillations*. In this case the equilibrium orbit is $x \equiv 0$ because it's the path we defined by the placement of the magnets and x represent only the deviation from this *ideal orbit*. For off-energy particles we must consider the perturbation term on the right hand side of the equation. This perturbation is a constant and generates a shift in the particle amplitudes from the ideal orbit. For example, particles with a higher than design energy $\delta > 0$ would oscillate about a path which is mostly outside ($x > 0$) of the ideal path and vice versa. The solution of the inhomogeneous equation of motion therefore defines the reference orbit for particles with energy $E = E_o(1 + \delta)$. Such particles perform oscillations about this reference orbit.

Solutions of the Equations of Motion

First, we set $\delta = 0$ and solve the homogeneous equation: $x'' + k(s)x = 0$. We cannot solve this equation in general since $k = k(s)$ is a function of $s$resembling the distribution of quadrupoles along the beam transport line. For $k > 0$ and $k =$const within a quadrupole, however, the solution is simply

$$\begin{aligned} x(s) &= a\,\cos(\sqrt{k}s) \,+\, b\sin(\sqrt{k}s) \\ x'(s) &= a\,-\sqrt{k}\sin(\sqrt{k}s) \,+\, b\sqrt{k}\cos(\sqrt{k}s) \end{aligned} \tag{20}$$

The integration constants a, b are determined by initial conditions: with $x = x_o$ and $x' = x'_o$ at $s = 0$, we get at point s

$$\begin{aligned} x &= x_o\cos(\sqrt{k}s) \,+\, x'_o\,\tfrac{1}{\sqrt{k}}\sin(\sqrt{k}s) \\ x' &= -x_o\sqrt{k}\,\sin(\sqrt{k}s) \,+\, x'_o\,\cos(\sqrt{k}s) \end{aligned} \tag{21}$$

These two equations express the particle position and slope at point s as a function of initial particle coordinates at $s = 0$.

Matrix Formalism

Both equations can be expressed in *matrix formulation*:

$$\begin{pmatrix} x \\ x' \end{pmatrix} = \begin{pmatrix} \cos(\sqrt{k}s) & \frac{1}{\sqrt{k}}\,\sin(\sqrt{k}s) \\ -\sqrt{k}\,\sin(\sqrt{k}s) & \cos(\sqrt{k}s) \end{pmatrix} \begin{pmatrix} x_o \\ x'_o \end{pmatrix} \tag{22}$$

For the case of a defocusing quadrupole $k < 0$ we derive a similar *transformation matrix*

$$\begin{pmatrix} x \\ x' \end{pmatrix} = \begin{pmatrix} \cosh(\sqrt{|k|}s) & \frac{1}{\sqrt{|k|}}\,\sinh(\sqrt{|k|}s) \\ \sqrt{|k|}\,\sinh(\sqrt{|k|}s) & \cosh(\sqrt{|k|}s) \end{pmatrix} \begin{pmatrix} x_o \\ x'_o \end{pmatrix} \tag{23}$$

A special case appears for $k = 0.0$ describing a drift space of length s for which the transformation matrix is

$$\begin{pmatrix} x \\ x' \end{pmatrix} = \begin{pmatrix} 1 & s \\ 0 & 1 \end{pmatrix} \begin{pmatrix} x_o \\ x'_o \end{pmatrix} \tag{24}$$

The transformations are expressed for quadrupoles of finite length. Sometimes it is desirable to perform quick calculations in which case we use the *thin lens approximation* just like in light optics by setting $s \to 0$ while $1/f = ks = $ const and get a thin lens transformation matrix for a quadrupole:

$$\begin{pmatrix} x \\ x' \end{pmatrix} = \begin{pmatrix} 1 & 0 \\ -\frac{1}{f} & 1 \end{pmatrix} \begin{pmatrix} x_o \\ x'_o \end{pmatrix} \tag{25}$$

Of course, in this case half the length of the quadrupole must be included to the drift space on either side.

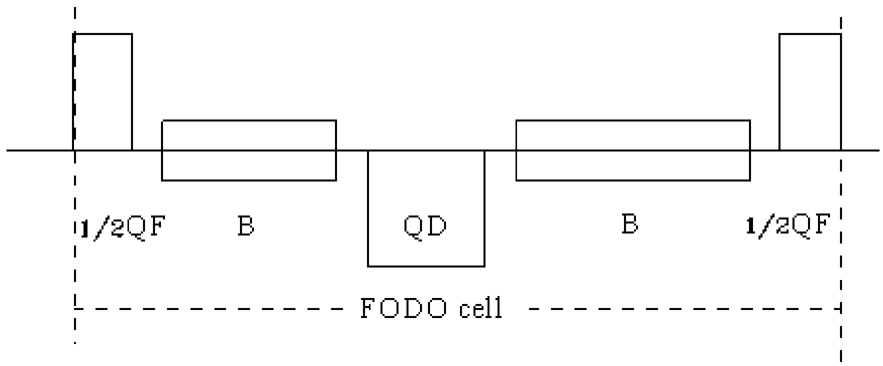

Figure 5: FODO Lattice schematic

Transformation of particle trajectories through complicated, multi-magnet arrangements, called *lattice*, with transformation matrices $M_1, M_2, \ldots$ are derived by simple matrix multiplication

$$M = M_n \cdot M_{n-1} \cdot \cdots \cdot M_2 \cdot M_1 \tag{26}$$

This matrix formalism is quite powerful and well matched to the capabilities of computers.

2.4 FODO Lattice

As an example of a beam line appropriate to demonstrate the usefulness of the matrix formalism we use what is called the FODO structure. This magnet structure consist of an alternating series of focusing and defocusing quadrupoles, thence the name FODO lattice as shown in Fig. 5. This lattice has been used to construct large high energy physics storage rings by filling the space between the quadrupoles with bending magnets. The FODO lattice is a very stable magnet configuration and its simplicity lends itself to "back-of-an-envelope" calculations.

To formulate particle dynamics in a FODO-lattice we keep the formalism simple by starting in the middle of a quadrupole. The transformation through a half cell, 1/2 QF - DRIFT - 1/2 QD, in thin lens approximation becomes

$$\begin{pmatrix} 1 - L/f_{\mathrm{f}} & L \\ -1/f^* & 1 - L/f_{\mathrm{d}} \end{pmatrix} = \begin{pmatrix} 1 & 0 \\ -1/f_{\mathrm{d}} & 1 \end{pmatrix} \begin{pmatrix} 1 & L \\ 0 & 1 \end{pmatrix} \begin{pmatrix} 1 & 0 \\ -1/f_{\mathrm{f}} & 1 \end{pmatrix} \tag{27}$$

where $1/f^* = 1/f_{\mathrm{f}} + 1/f_{\mathrm{d}} - L/(f_{\mathrm{f}}\, f_{\mathrm{d}})$. For the second half cell we get the transformation matrix by replacing $f_{\mathrm{f}} \rightarrow f_{\mathrm{d}}$ and vice versa. For simplicity we consider a symmetric FODO lattice by setting $f_{\mathrm{f}} = -f_{\mathrm{d}} = f$ and get by multiplying the half cell transformation matrices the transformation matrix of a full FODO-cell starting in the center of a QF and ending in the middle of the next QF:

$$M_{\mathrm{cell,qf}} = \begin{pmatrix} 1-2L^2/f^2 & 2L(1+L/f) \\ -2L/f^2(1-L/f) & 1-2L^2/f^2 \end{pmatrix} \tag{28}$$

This transformation matrix is valid for the horizontal plane. In the vertical plane we have the same matrix except that the sign of the focal length must be changed: $f \to -f$.

We may combine the transformation in both planes into one 4×4 transformation matrix which we can use to transform a particle trajectory with initial coordinates x_o, x'_o, y_o, y'_o to the end of the FODO-cell.

$$\begin{pmatrix} x \\ x' \\ y \\ y' \end{pmatrix} = \begin{pmatrix} 1-2\frac{L^2}{f^2} & 2L(1+\frac{L}{f}) & 0 & 0 \\ -2\frac{L}{f^2}(1-\frac{L}{f}) & 1-2\frac{L^2}{f^2} & 0 & 0 \\ 0 & 0 & 1-2\frac{L^2}{f^2} & 2L(1-\frac{L}{f}) \\ 0 & 0 & -2\frac{L}{f^2}(1+\frac{L}{f}) & 1-2\frac{L^2}{f^2} \end{pmatrix} \begin{pmatrix} x_o \\ x'_o \\ y_o \\ y'_o \end{pmatrix} \tag{29}$$

For practical reasons, however, mostly only 2×2 matrices are used to describe the dynamics in one plane only.

2.5 Betatron Function

Although the quadrupole strength is a function of s, $k = k(s)$, the homogeneous part of the equation of motion(19) looks very much like that of a harmonic oscillator $x'' + k(s)x = 0$. As an analytical solution of the equation of motion we try the ansatz

$$x(s) = a_i \sqrt{\beta(s)} \cos(\psi(s) + \varphi_i) \tag{30}$$

where a_i and φ_i are the integration constants for particle i and $\beta(s)$ and $\psi(s)$ are so far unidentified functions of s. We insert this ansatz into the differential equation and by sorting the sine- and cosine-terms we get two conditions for $\beta(s)$ and $\psi(s)$

$$\frac{\mathrm{d}^2\sqrt{\beta}}{\mathrm{d}s^2} + k(s)\sqrt{\beta} + \beta^{-\frac{3}{2}} = 0 \tag{31}$$

$$\psi'(s) = \frac{1}{\beta(s)} \tag{32}$$

where the primes $'$ are derivations with respect to s.

Equation (30) describes the oscillatory motion of particles about a reference orbit, here the ideal orbit leading through the center of all magnets. These oscillations are defined separately in both the horizontal and vertical plane and are called *betatron oscillations*. The function $\beta(s)$ is called the *betatron function* and is defined by the placement and strength of the quadrupole magnets. It is a periodic function of s resembling the periodic distribution of quadrupoles on the ring circumference. The periodicity is the circumference of the machine or shorter if quadrupoles are arranged around the ring in a higher periodicity.

Because of the nonlinearity of the differential equation for the betatron function there is only one periodic solution in each plane for a given lattice configuration. Matrix formalism is used to determine this one betatron function in each plane utilizing special computer programs. For each lattice configuration a tabulated list of the values of betatron functions exists which can be used to determine beam sizes. The betatron function is, however, of much higher importance in beam dynamics beyond the ability to calculate single particle trajectories as we will discuss in the next section.

Betatron Phase and Tune

The second equation (32) can be integrated immediately for

$$\psi(s) \;=\; \int_o^s \frac{\mathrm{d}\sigma}{\beta(\sigma)} \tag{33}$$

generating the phase of the betatron oscillation at point s and measured from the starting point $s = s_o$. Integration all along the ring orbit produces the *tune* $\nu_{x,y}$ of the machine which is equal to the number of betatron oscillations per orbit. Again, tunes are defined separately in both planes.

$$\nu_{x,y} \;=\; \frac{\psi_{x,y}(C)}{2\pi} \;=\; \frac{1}{2\pi} \oint \frac{\mathrm{d}\sigma}{\beta_{x,y}(\sigma)} \tag{34}$$

The significance of the tune is that it may not be an integer or a half integer. If one or the other assumes such a value beam dynamics becomes instantly unstable leading to beam loss. This becomes obvious for an integer resonance ($\nu_{x,y} = n$) considering a small dipole field perturbation at say one point along the orbit. this dipole field gives the beam a transverse kick at the same phase of its betatron oscillations after every turn building up larger and larger oscillation amplitudes until the beam gets lost on the vacuum chamber walls.

Beam Envelope

Solution (30) describes individual particle trajectories all differing by different amplitudes a_i and phases φ_i. If we choose only particles with the largest amplitude $a_i = \hat{a}$ within the beam and further look among those particles for the one for which $\cos(\psi(s) + \varphi_i) = 1$ we have defined the *beam envelope* at point s:

$$E_{x,y}(s) \;=\; \pm\, \hat{a}_{x,y} \sqrt{\beta_{x,y}(s)} \tag{35}$$

No other particle will have a greater amplitude at this point. Knowledge of the betatron functions in both the x and y-plane and knowledge of the quantity $\hat{a}$ in both planes will allow us to define the beam dimensions at any point along the ring orbit. The quantity $\hat{a}$ is actually what we generally call the *beam emittance*,

$\epsilon_{x,y} = \hat{a}^2$. Since in a storage ring the particle distribution in 6-dim phase space is Gaussian we cannot define a maximum beam size and the beam emittance is therefore defined for the one-sigma particles of the Gaussian distribution.

$$\epsilon_{\sigma,u} = \frac{\langle u^2 \rangle}{\beta_u} = \tfrac{1}{2}\langle a_i^2 \rangle \tag{36}$$

where u stands for x or y respectively.

As important the knowledge of the beam width and height at some point s is we do not yet have the tools to calculate either the numerical value of the betatron functions nor that of the beam emittances in bot the horizontal and vertical plane. This we will do in the next lecture.

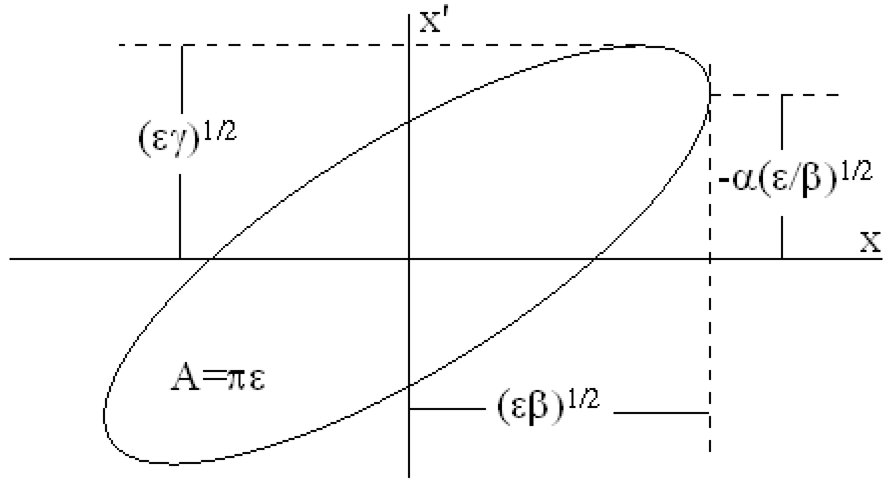

Figure 6: Phase Space Ellipse

3 Beam Optics

The matrix formulation is a very powerful tool to calculate the trajectories of single particles. Yet, in a storage ring there are of the order of 10^{11} or more particles circulating and it would be prohibitive to have to calculate the trajectories of all particles anytime a quadrupole strength is changed. We are looking therefore for a simpler formalism which allows us to determine the behavior of a multi-particle beam.

3.1 Phase Ellipse

Particles perform oscillatory motion, called *betatron oscillations*, about the ideal reference orbit and its amplitude and slope is given by

$$\begin{aligned} x &= a\sqrt{\beta(s)}\,\cos(\psi(s)+\varphi) \\ x' &= -a\frac{\alpha}{\sqrt{\beta(s)}}\cos(\psi(s)+\varphi) - a\sqrt{\beta(s)}\sin(\psi(s)+\varphi)\cdot\psi' \end{aligned} \tag{37}$$

where $\alpha = -\frac{1}{2}\beta'$ and $\gamma = \frac{1+\alpha^2}{\beta}$. All quantities α, β and γ are defined in x and y and are known as *betatron functions* or *lattice functions*. Eliminating the phase $\psi(s)+\varphi$ from both equations we get a constant of motion

$$\gamma x^2 + 2\alpha x x' + \beta x'^2 = a^2 \tag{38}$$

This equation describes an ellipse, the phase space ellipse (Fig:6) with area πa. Individual particles travel along an ellipse, the *phase ellipse* in (x, x')-or

$(y, y')-$phase space defined by amplitudes a_i different for each particle. The functions $\alpha(s), \beta(s)$,and $\gamma(s)$ are called *lattice functions* defined separately both for x and y.

Due to *Liouville's theorem* which states that in the presence of only external macroscopic fields as we have in storage rings the particle density in phase space is a constant of motion. That means no particle can cross the phase ellipse of any other particle. We may therefore look for the particles with the maximum amplitude $\hat{a}$ travelling along an ellipse which encloses all other particles. This phase ellipse then becomes representative for the whole beam. We have thereby succeeded in describing the dynamics of a many-particle beam by the dynamics of a single particle. Due to the variation of the betatron functions along the orbit the phase ellipses also change their form and orientation but the area of the phase ellipses stays constant. At a particular point s the phase ellipse has always the same shape/orientation while the particle jumps appears on the ellipse at different points anytime it completes an orbit.

The constant $\pi\hat{a}$ is the area of the largest phase ellipse in a beam and we use this area to define the *beam emittance* by $\frac{1}{2}\,\hat{a}^2 = \epsilon$. Because of synchrotron radiation, an electron beam in a storage ring has a *Gaussian distribution* and it is customary to define the beam emittance for a Gaussian particle distribution by the amplitude of the one-sigma particle

$$\epsilon_x = \frac{\langle x_\sigma^2 \rangle}{\beta_x(s)} = \frac{\sigma_x^2}{\beta_x(s)} \tag{39}$$

The standard beam size is then defined by:

$$\sigma_x = \sqrt{\epsilon_x \beta_x} \qquad \text{and} \qquad \sigma_y = \sqrt{\epsilon_y \beta_y} \tag{40}$$

and the beam divergence by:

$$\sigma_{x'} = \sqrt{\epsilon_x \gamma_x} \qquad \text{and} \qquad \sigma_{y'} = \sqrt{\epsilon_y \gamma_y}\,. \tag{41}$$

Ignoring for the moment effects due to the finite energy spread in the beam and diffraction , the photon source parameters in transverse phase space are defined and equal to the electron beam in both cross section and divergence.

$$\text{electron beam parameters } \equiv \text{photon beam parameters}$$

3.2 Variation of the Phase Ellipse

While the area of the phase ellipse is a constant of motion, the shape of the ellipse is not. The orientation and aspect ratio continuously change through the action of quadrupol focusing and even along a fieldfree drift space. In Fig. 7 the variation of the phase ellipse is shown for a beam in a drift space while converging to a minimum followed by divergence.

The phase ellipse for a converging beam is tilted to the left while that for a diverging beam is tilted to the right. Of special interest is the *upright ellipse*

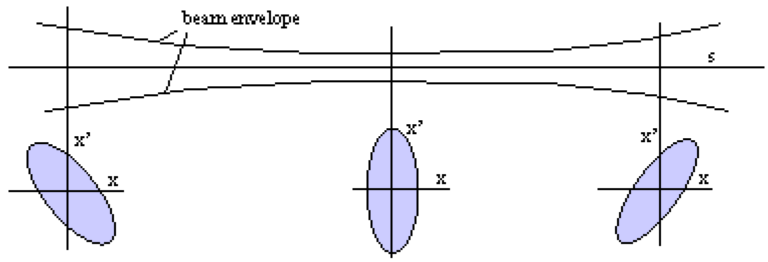

Figure 7: Variation of a Phase Space Ellipse along a Drift Space

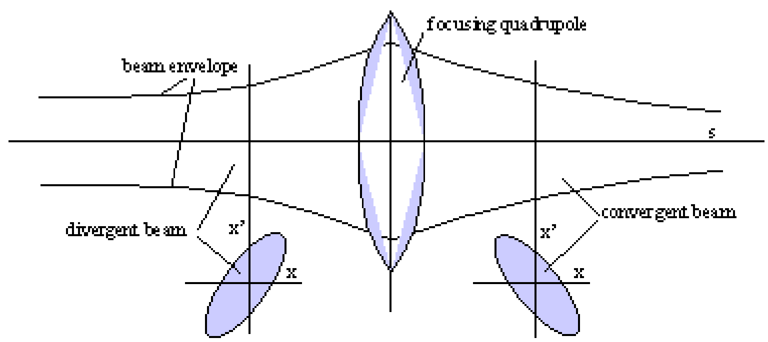

Figure 8: Evolution of a Phase Ellipse within a Quadrupole Magnet

which occurs at any symmetry point. At such a point $\alpha_{x,y} = 0$ and $\gamma_{x,y} = 1/\beta_{x,y}$. Fig 8 shows the variation of the phase ellipse as the beam travels through a focusing quadrupole.

3.3 Transformation of Betatron Functions

The transformation matrix for a single particle can be used to determine the transformation of the phase ellipse from one point to another. *Liouville's theorem* requires that

$$\gamma x^2 + 2\alpha x x' + \beta {x'}^2 \;=\; \gamma_o x_o^2 + 2\alpha_o x_o {x'}_o + \beta_o {{x'}_o}^2 \;=\; a^2 \qquad (42)$$

Particle coordinates $(x_o, {x'}_o)$ and (x, x') are related by the transformation matrix $M = \begin{pmatrix} a & b \\ c & d \end{pmatrix}$. Replacing coordinates (x_o, x'_o) by (x, x') and collecting coefficients for x^2, ${x'}^2$ and xx' we obtain a relation of the betatron functions from one point to another noting that the coordinates are independent variables and therefore the coefficients must cancel individually. In matrix formulation the transformation of betatron functions is given by from the and ordering we get for the transformation of the coefficients:

$$\begin{pmatrix} \beta \\ \alpha \\ \gamma \end{pmatrix} = \begin{pmatrix} a^2 & -2ab & b^2 \\ -ac & ad+bc & -bd \\ c^2 & -2cd & d^2 \end{pmatrix} \begin{pmatrix} \beta_o \\ \alpha_o \\ \gamma_o \end{pmatrix} = M_\beta \cdot \begin{pmatrix} \beta_o \\ \alpha_o \\ \gamma_o \end{pmatrix} \tag{43}$$

The transformation of betatron functions can be expressed by the elements of the single particle transformation matrices.

3.4 Periodic Betatron Function

In circular accelerators we require that the betatron functions at point s are the same from turn to turn and therefore $\vec{\beta} = M_\beta \, \vec{\beta}_o = \vec{\beta}_o$. This periodic solution of the betatron functions can be derived from the eigenvalues of the eigenfunction equation

$$(M_\beta - I)\vec{\beta} = 0\,, \tag{44}$$

where M_β is the transformation matrix from point s through a whole orbit to point $s + C$, C the ring circumference and I is the unit matrix.

Generally, storage rings are composed of a number of equal sections with the same magnet distribution. In this case each section, called either *cell* or *unit* is representative for all cells and we need to find the periodic solution for this cell only. this solution then repeats as we progress along the orbit.

3.4.1 Periodic Betatron Function in a FODO Lattice

As an example, we look for the periodic solution of the betatron function in a FODO lattice. With $\alpha_o = 0; \gamma_o = 1/\beta_o$ in the middle of the QF we solve for the periodic betatron function $\beta = \beta_o = (1 - 2L^2/\,f^2)^2\beta_o + 4L^2(1 + L/\,f)^2/\beta_o$. Similarly we can go from the middle of the QD to the middle of the next QD and get the value of the periodic betatron function in the middle of the QD. Since a QF is a QD in the vertical plane and vice versa the two solutions just described present the value of the horizontal and vertical betatron function in the middle of the QF and interchangeably those in the middle of the QD. With $\varkappa = f/L$ these values of the betatron functions are in the middle of the QF

$$\beta_{x,o} = L\frac{\varkappa(\varkappa+1)}{\sqrt{\varkappa^2-1)}} \qquad \text{and} \quad \beta_{y,o} = L\frac{\varkappa(\varkappa-1)}{\sqrt{\varkappa^2-1)}} \tag{45}$$

For the values in the middle of the QD interchange x with y. Obviously, a solution and therefore beam stability exists only if $\varkappa > 1$ or if $f > L$! Knowing

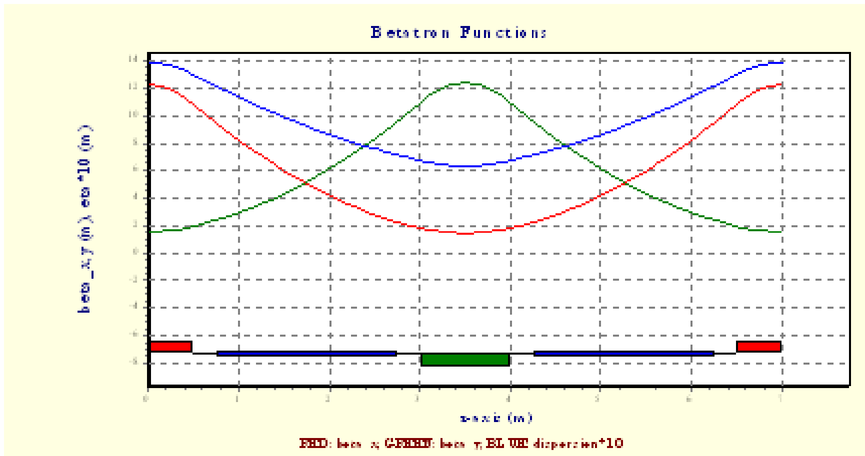

Figure 9: Betatron Functions in a FODO-Lattice

the betatron functions at one point is enough to allow the calculation of those functions at any other point in the lattice. In Fig. 9 the betatron functions are shown for one cell of a FODO lattice. Note the similarity of the horizontal and vertical betatron functions being only one quadrupole distance shifted with respect to each other. The periodic nature of the solutions which allows us to use such a FODO lattice to construct a circular accelerator with a repetition of cells, betatron functions and beam sizes.

3.5 Dispersion Function

So far we have treated particle dynamics for a monochromatic beam only and the solutions for particle trajectories cover only those of the homogeneous differential equation of motion. This is not correct for a real beam and we must consider corrections due to effects of energy errors. Chromatic effects are described by a particular solution of the inhomogeneous differential equation

$$x''_\delta + kx_\delta = \frac{1}{\rho_o}\delta \tag{46}$$

where $\delta = \Delta E/E_o$. The general solution is $x = x_\beta + x_\delta$, where the betatron oscillation is x_β is the solution of the homogeneous differential equation and x_δ the offset for off-momentum particles. The particular solution x_δ describes the reference path about which particles perform betatron oscillations x_β. For $\delta = 0$ this reference path is $x_\delta \equiv 0$ which is the trivial solution since we placed the magnets along this path. For $\delta \neq 0$ we get solutions for the reference path of off-momentum particles. The reference path x_δ scales linear with δ and we may therefore define a function $\eta(s) = x_\delta(s)/\delta$ which is called the *dispersion function* or *η-function*. Like the betatron functions there is only one periodic solution for the dispersion function an example of which is show in Fig. 9 for a FODO cell. The values for this function are generally calculated and listed by appropriate computer programs together with the betatron functions. Like the betatron functions, the dispersion function is actually not determined by solving the inhomogeneous differential equation but rather by matrix formalism.

For any energy deviation δ we have now a different reference path about which particles with this energy deviation perform betatron oscillations. The η-function varies generally between zero and positive values. Particles with $\delta > 0$ follow therefore a path which is farther away from the ring center while lower energy particles follow a path closer to the ring center than the ideal orbit. The length of the closed path is therefore also energy dependent which becomes of greater importance later in connection with synchrotron oscillations discussed in the next.

3.5.1 Dispersion or η-Function in a FODO Lattice

To construct a storage ring made up of FODO cells we place bending magnets between the quadrupoles. For off-energy particles these bending magnet cause a shift of the reference orbit through the solution of the inhomogeneous equation of motion. The scaling of the shift is described by the η-function and the actual shift is the $\eta(s)\delta$. It is significant to note that similar to the betatron functions in the x- and y-plane the η-function too has only one solution for a given lattice. It can be calculated in a similar fashion as the betatron function by use of the matrix formalism. Without proof, the periodic η-function becomes in thin lens approximation in the middle of the QF- and QD-quadrupole

$$\eta_{\mathrm{qf}} = \frac{L^2}{2\rho}\varkappa(2\varkappa+1) \qquad \text{and} \qquad \eta_{\mathrm{qd}} = \frac{L^2}{2\rho}\varkappa(2\varkappa-1) \tag{47}$$

Knowing the η-function at one point allows us to calculate its values at any other point around the storage ring and the result for a FODO lattice is shown in Fig. 9.

With the addition of these chromatic effects the total beam size is modified like

$$\sigma_{x_{\mathrm{tot}}} = \sqrt{\epsilon_x\beta_x + \eta^2\delta^2} \qquad \text{and} \qquad \sigma_y = \sqrt{\epsilon_y\beta_y} \tag{48}$$

where $\delta = \delta E/E_o$ is the relative energy spread in the beam. The total beam divergence is

$$\sigma_{x'_{\mathrm{tot}}} = \sqrt{\epsilon_x\gamma_x + \eta'^2\delta^2} \qquad \text{and} \qquad \sigma_{y'} = \sqrt{\epsilon_y\gamma_y} \tag{49}$$

There is no effect on the vertical beam parameters since we assume a storage ring with only horizontal bending magnets.

4 Radiation Effects

Particle dynamics is greatly influenced by the emission of radiation as well as by the restoration of the energy loss in accelerating cavities. These processes are both beneficial and perturbative and fundamentally determine the electron beam parameters and thereby the characteristics of the photon beam. We will here briefly discuss these effects to illuminate the basic physics responsible for the photon beam characteristics in a synchrotron light source.

4.1 Radiation Power

As electrons travel through magnetic fields they experience a Lorentz force which deflects the beam orthogonal to the field and velocity vector(see lecture on Synchrotron radiation). This force is the cause for the emission of electromagnetic radiation. The instantaneous radiation power is given by

$$P_\gamma(\mathrm{GeV/sec}) = \frac{cC_\gamma}{2\pi}\frac{E^4(\mathrm{GeV})}{\rho^2(\mathrm{m})} \tag{50}$$

where

$$C_\gamma = \frac{4\pi}{3}\frac{r_\mathrm{c}}{(mc^2)^3} = 8.8575 \cdot 10^{-5}\mathrm{m/GeV}^3 \tag{51}$$

The rate of energy loss to synchrotron radiation is proportional to the square of the particle energy and magnetic field strength in the bending magnets ($B \propto E/\rho$). We may integrate this radiation power all around the ring to get the total energy loss per turn, U_o, into synchrotron radiation. For a ring composed of a set of equal magnets with the same curvature $1/\rho$ this integration can be performed generally and is with $U_o = \oint P_\gamma \mathrm{d}t = \oint P_\gamma \mathrm{d}s/c$

$$U_o(\mathrm{GeV}) = C_\gamma \frac{E^4(\mathrm{GeV})}{\rho(\mathrm{m})} \tag{52}$$

This loss of energy into synchrotron radiation during each revolution while small compared to the electron energy is still a strong enough perturbation that must be compensated.

4.2 Synchrotron Oscillations

One or more rf-cavities are located along the orbit of the ring. These cavities are excited by external microwave sources to generate electric fields parallel to the beam path through the cavity providing the acceleration needed to compensate for this energy loss. Since the rf-fields oscillate very fast (order of 500 MHz) the particle arrival time at the cavity is very critical (Fig. 10). On the other hand, we notice that particles with higher than ideal energy follow a path with mostly larger average radius while particle with smaller energies follow a path mostly inside of the ideal path at smaller radii. All particles are highly relativistic, travel close to the speed of light and the going around travel time depends therefore on the particle energy. We still can get a stable beam due to the feature of *phase focusing* which forces particles to arrive at the cavity, if not exactly at a specific phase of the accelerating field, at least close to the exact or *synchronous phase/time*. Nonideal particles are made to oscillate about the ideal parameters

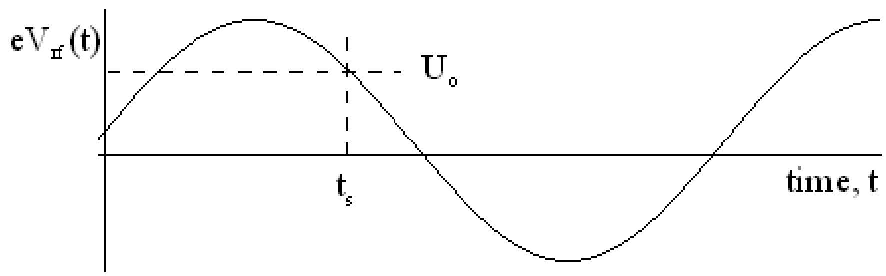

Figure 10: Cavity rf-voltage

similar to betatron oscillation of particles under the field of quadrupole magnets about the ideal orbit. These oscillations are called *synchrotron oscillations*.

To formulate this phase focusing we consider the total energy change per turn $\mathrm{d}E = eV_{\mathrm{rf}}(t) - U(E)$, where $V_{\mathrm{rf}}(t)$ is the rf-voltage at the time t and $U(E)$ the energy loss per turn at energy E. We define the ideal energy E_o and synchronous time t_{s} at which the ideal particle would gain an energy exactly equal to the lost energy. Expanding at $t = t_{\mathrm{s}} + \tau$ and $E = E_o + \varepsilon$ keeping only linear terms and dividing by the revolution time T_o we get:

$$\begin{aligned} \frac{\mathrm{d}\varepsilon}{\mathrm{d}t} &= \frac{1}{T_o}\left[eV_{\mathrm{rf}}(t_{\mathrm{s}}) + e\frac{\partial V_{\mathrm{rf}}}{\partial t}|_{t_{\mathrm{s}}}\,\tau - U(E_o) - \frac{\mathrm{d}U}{\mathrm{d}E}|_{E_o}\,\varepsilon\right] \\ &= \frac{1}{T_o}\left[e\frac{\partial V_{\mathrm{rf}}}{\partial t}|_{t_{\mathrm{s}}}\,\tau - \frac{\mathrm{d}U}{\mathrm{d}E}|_{E_o}\,\varepsilon\right] \end{aligned} \tag{53}$$

where we made use of the fact that $eV_{\mathrm{rf}}(t_s) = U(E_o)$.

On the other hand, the revolution time depends on the particle velocity and momentum dependent path length (α_c *momentum compaction factor*). The revolution time for a particle with energy deviation ε is different the ideal revolution time T_o and we find with $\Delta T/T_o = \mathrm{d}\tau/\mathrm{d}t$

$$\frac{\mathrm{d}\tau}{\mathrm{d}t} = (\gamma^{-2} - \alpha_c)\frac{\varepsilon}{E_o} \tag{54}$$

The $1/\gamma^2$-term is due to the velocity variation with energy and the momentum compaction factor is defined by the ratio of the relative change of the orbital path length to the relative energy error, $\Delta C/C_o = \alpha_{\mathrm{c}}\Delta E/E_o$ and is $\alpha_{\mathrm{c}} = \langle\eta/\rho\rangle_{\mathrm{s}}$ averaged over all circumference.

Differentiation of (53) with respect to t and replacing $\dot{\tau}$ by (54) we get the equation of motion for *synchrotron oscillations*

$$\frac{\mathrm{d}^2\varepsilon}{\mathrm{d}t^2} + 2\alpha_s\frac{\mathrm{d}\varepsilon}{\mathrm{d}t} + \omega_{\mathrm{s}}^2\varepsilon = 0 \tag{55}$$

where we have defined the damping decrement for synchrotron oscillations by

$$\alpha_{\mathrm{s}} = \frac{1}{2T_o}\frac{\mathrm{d}U(E_o)}{\mathrm{d}E} = \frac{1}{2}\frac{\mathrm{d}\langle P_\gamma\rangle}{\mathrm{d}E} = 2\frac{\langle P_\gamma\rangle}{E_o} \tag{56}$$

The synchrotron radiation power $\langle P_\gamma \rangle$ is the average over all circumference and the synchrotron oscillation frequency ω_{s} is with $\omega_o = 2\pi/T_o$

$$\omega_{\mathrm{s}}^2 = \frac{(\gamma^{-2} - \alpha_{\mathrm{c}})}{E_o T_o} e \frac{\mathrm{d}V(t)}{\mathrm{d}t} = \omega_o^2 \frac{h(\gamma^{-2} - \alpha_{\mathrm{c}}) e V_o \cos\psi_{\mathrm{s}}}{2\pi E_o} \tag{57}$$

Here we made use of the fact that the integrated rf-field changes sinusoidally with time like $V_{\mathrm{rf}} = V_o \sin\omega_{\mathrm{rf}} t$ and therefore $\dot{V} = \omega_{\mathrm{rf}} V_o \cos\psi_{\mathrm{s}} = 2\pi h/T_o V_o \cos\psi_{\mathrm{s}}$ where h is the harmonic number which is defined by $h = C_o/\lambda_{\mathrm{rf}}$ and must be integer and $\psi_{\mathrm{s}} = \omega_{\mathrm{rf}} t_{\mathrm{s}}$ is the synchronous phase at which a particle with energy E_o is accelerated exactly to compensate for the energy loss to radiation.

The differential equation of motion exhibits two significant terms; for one, we may expect stable synchrotron oscillations with frequency ω_{s} only if the synchronous phase is chosen such that this frequency is real and not imaginary; furthermore, the damping term tells us that any deviation of a particle from the ideal parameters in longitudinal phase space is damped away due to the emission of synchrotron radiation; One deviation may be the particle energy. Due to the fact that synchrotron radiation depends on the particle energy in such a way that higher/lower energy particles loose more/less energy we observe an energy correcting effect of the emission of synchrotron radiation.

The solution to the differential equation of motion is that of a damped harmonic oscillator

$$\varepsilon(t) = \varepsilon_o \, \mathrm{e}^{-\alpha_{\mathrm{s}} t} \, \mathrm{e}^{\mathrm{i}\omega_{\mathrm{s}} t} \tag{58}$$

Generally, the damping time $\tau_s = 1/\alpha_s$ is of the order of msec's while the synchrotron oscillation time is much shorter of the order of 10 - 50 μ-sec. This different time scale allows us to treat synchrotron oscillations while ignoring damping.

While the particles obit the storage ring they perform oscillations in energy about the ideal energy E_o. At the same time there is also an oscillation about the synchronous time described by τ. which from (54) is 90° out of phase. This longitudinal oscillation about the synchronous time t_{s} leads to a longitudinal distribution of particles and defines the bunch length. Later we will quantify this bunch length. The energy spread in the beam is therefore directly related to the bunch length and the bunch length defines the pulse length of the photon pulse from each electron bunch.

4.3 Damping

Due to synchrotron radiation all coordinates in 6-dim $(x, x', y, y', \Delta E, \tau)$ phase space are being damped. As we have seen above, energy damping occurs at a rate proportional to synchrotron radiation power P_γ.

Damping occurs also in the transverse plane due to a geometric effect. While particles perform betatron oscillations they emit radiation generally at a finite angle with the beam axis. During this emission of radiation the particles loose

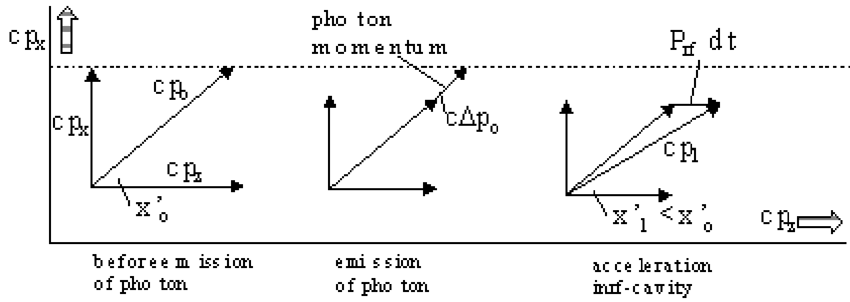

Figure 11: Transverse Damping Effects

longitudinal as well as transverse momentum. Yet, in the rf-cavity acceleration occurs only in the longitudinal direction. As a consequence, the combined process of emission and acceleration results in a net loss of transverse momentum which is equivalent to a reduction in the betatron amplitude and constitutes thereby transverse damping.

To be more quantitative, we note that the direction of the particle motion does not change with the emission of radiation since radiation is emitted in the forward direction within a very small angle of $1/\gamma$. Right after emission of a photon the transverse momentum is $(cp_o - c\Delta p)\, x'_o$. This transverse momentum will not be changed by the acceleration in the rf-cavity which we assume for simplicity to occur at the location of the radiation emission and we have then

$$(cp_o - c\Delta p)\, x'_o \;=\; (cp_o - c\Delta p + P_{\mathrm{rf}}\mathrm{d}t)\, x'_1 \tag{59}$$

where x'_o, x'_1 are the angles of the particle trajectories with respect to the beam axis before and after acceleration, respectively and the acceleration is equal to the energy loss, $P_{\mathrm{rf}}\mathrm{d}t = P_\gamma \mathrm{d}t$ (Fig. 11.

With $x' = \dot{x}/\beta c$ and E the particle energy after emission of a photon but before acceleration we get

$$\dot{x}_1 \;=\; \frac{E}{E + P_\gamma \mathrm{d}t}\dot{x}_o \;\approx\; \left(1 - \frac{P_\gamma \mathrm{d}t}{E}\right)\dot{x}_o \tag{60}$$

The difference between E and E_o is very small and the horizontal damping decrement is then

$$\alpha_x = -\frac{1}{\dot{x}_o}\frac{\mathrm{d}\dot{x}}{\mathrm{d}t} = \frac{P_\gamma}{E_o} \tag{61}$$

A similar expression is valid for the vertical plane:

$$\alpha_y = -\frac{1}{\dot{y}_o}\frac{\mathrm{d}\dot{y}}{\mathrm{d}t} = \frac{P_\gamma}{E_o} \tag{62}$$

Because of this damping the betatron oscillation $x(t) = A(t)\sqrt{\beta}\cos\psi(t)$ scales with time like

$$A(t) \;=\; A_o(t)\mathrm{e}^{-\alpha_\mathrm{s} t} \tag{63}$$

Under certain circumstances one or more damping decrements may be modified, e.g. when we have a field gradient in a bending magnet. However, due to very general principles the sum of all damping decrements is a constant:

$$\alpha_s + \alpha_x + \alpha_y \;=\; 4\frac{P_\gamma}{E_o} \tag{64}$$

Whenever one decrement is modified another will be modified as well. From here on we will ignore such details and point to more detailed discussions on this point to available literature.

4.4 Quantum Effects

Damping of 6-dim phase-space coordinates is counterbalanced in a storage ring by what is called quantum effects. This is a misnomer since emission of synchrotron radiation is a completely classical process. What is meant is this, the emission of electromagnetic radiation in say one bending magnet occurs during such a short time (the time it take the particle to travel through the magnet) that the particle cannot react adiabatically to the perturbation created by this radiation emission. The particle reaction time scales are actually the damping times. Therefore we have to deal with events that seem to happen suddenly.

Consider, for example, a particle i performing synchrotron oscillations: $A = A_o\mathrm{e}^{\mathrm{i}\omega_\mathrm{s}(t-t_o)}$ where we assume that the last emission of radiation occurred at time t_o. New radiation with total energy ε_rad is emitted at time t_1. To simplify the mathematics we break up this radiation into individual photons with energy ε. Each emission of a photon causes an energy jump in phase space and the synchrotron oscillation is altered like:

$$\begin{aligned} A &= A_o \exp\left[\mathrm{i}\omega_\mathrm{s}(t-t_o)\right] - \varepsilon \exp\left[\mathrm{i}\omega_\mathrm{s}(t-t_1)\right] \\ &= A_1 \exp\left[\mathrm{i}\omega_\mathrm{s}(t-t_1)\right] \end{aligned} \tag{65}$$

Solving for new amplitude we get

$$A_1^2 \;=\; A_o^2 + \varepsilon^2 - 2\varepsilon A_o \cos[\omega_\mathrm{s}(t_1 - t_o)] \tag{66}$$

Radiation emission occurs many times during a synchrotron oscillation period and we may therefore average over all times to get the average change in the oscillation amplitude due to the emission of a photon with energy ε.

$$\langle \delta A^2 \rangle \;=\; \langle A_1^2 - A_o^2 \rangle \;=\; \langle \varepsilon^2 \rangle \tag{67}$$

Furthermore, we average now over all photon energies in the radiation spectrum and get the rate of change of the synchrotron oscillation amplitude

$$\left\langle \frac{\mathrm{d}A^2}{\mathrm{d}t} \right\rangle_{s,\mathrm{excitation}} = \int_o^\infty \varepsilon^2 \dot{n}(\varepsilon)\,\mathrm{d}\varepsilon \;=\; \langle \dot{N}_\mathrm{ph} \langle \varepsilon^2 \rangle \rangle_s \tag{68}$$

where $\dot{n}$ is the number of photons of energy ε emitted per unit time and $\dot{N}_{\mathrm{ph}}$ is the total number of all photons emitted per unit time. The subscript s indicates that the integral be taken along the circumference of the ring. Since both photon energy and flux are positive we have from this effect a continuous increase of the oscillation amplitude.

4.5 Equilibrium Beam Parameters

Two effects act on the particle beam, damping and quantum excitation which eventually determine the transverse beam sizes, beam divergencies, energy spread and bunch length. Adding both growth rates leads to an equilibrium value of any of these quantities.

4.5.1 Equilibrium Energy Spread

Equilibrium quantities can be derived by combining the quantum excitation (68) with damping

$$\left\langle \frac{\mathrm{d}A^2}{\mathrm{d}t} \right\rangle_{s,\mathrm{excitation}} + \left\langle \frac{\mathrm{d}A^2}{\mathrm{d}t} \right\rangle_{s,\mathrm{damping}} = 0 \tag{69}$$

where $\left\langle \frac{\mathrm{d}A^2}{\mathrm{d}t} \right\rangle_s |_{\mathrm{damping}} = -2\alpha_s \langle A^2 \rangle$. With $\tau_s = 1/\alpha_s$ we get

$$\langle A^2 \rangle = \tfrac{1}{2}\tau_s \langle \dot{N}_{\mathrm{ph}} \langle \varepsilon^2 \rangle \rangle_s \tag{70}$$

where $\dot{N}_{\mathrm{ph}}\langle \varepsilon^2 \rangle = \frac{55}{24\sqrt{3}} \left[cC_\gamma \hbar c (mc^2)^4 \right] \gamma^7/\rho^3$. The Gaussian energy spread is defined by $\sigma_\varepsilon^2 = \frac{1}{2}\langle A^2 \rangle$ and the equilibrium energy spread is

$$\left(\frac{\sigma_\varepsilon}{E} \right)^2 = C_q \frac{\gamma^2 \langle 1/\rho^3 \rangle}{2\langle 1/\rho^2 \rangle} \tag{71}$$

where

$$C_q = \frac{55}{32\sqrt{3}} \frac{\hbar c}{mc^2} = 3.84 \times 10^{-13}\,\mathrm{m} \tag{72}$$

For an isomagnetic ring, where all bending magnets are of the same strength the energy spread is

$$\left(\frac{\sigma_\varepsilon}{E} \right)^2 = C_q \frac{\gamma^2}{2\rho} \tag{73}$$

4.5.2 Bunch Length

The energy oscillation is correlated with a longitudinal oscillation about the bunch center and a beam with a Gaussian energy spread will have also a Gaussian longitudinal distribution. From (54) we have $\omega_{\mathrm{s}}\sigma_\tau = |(\gamma^{-2} - \alpha_c)| \frac{\sigma_\varepsilon}{E_o}$ and the bunch length $\sigma_\ell = \frac{c|(\gamma^{-2}-\alpha_c)|}{\omega_{\mathrm{s}}} \frac{\sigma_\varepsilon}{E_o}$ noting that $\sigma_\ell = c\sigma_\tau$. Replacing the synchrotron oscillation frequency by its definition (57) we get finally for the equilibrium bunch length

$$\sigma_\ell = \frac{\sqrt{2\pi}c}{\omega_{\text{rev}}}\sqrt{\frac{|(\gamma^{-2}-\alpha_c)|E_o}{he\hat{V}_{\text{rf}}\cos\psi_s}}\,\frac{\sigma_\varepsilon}{E_o} \tag{74}$$

The bunch length is proportional to the energy spread and can be reduced in principle by increasing the rf-voltage although the reduction scales only like the square root.

4.5.3 Horizontal Beam Emittance

Similar to the beam energy spread we find an emittance increasing excitation effect also in transverse phase space. The emission of radiation occurs in a time short compared to the damping time and therefore causes a sudden change in the particle energy and consequently a sudden change of its reference orbit. Since the electron cannot jump to the new reference orbit it must oscillate about it with a new betatron amplitude. The particle position is the sum of the betatron amplitude and the offset due to is energy deviation. Emission of a photon with energy ε cannot cause a change in the particle position x but rather a variation of its components

$$\begin{array}{lcll} \delta x & = & 0=\delta x_\beta+\eta\frac{\varepsilon}{E_o} & \rightarrow \quad \delta x_\beta=-\eta\frac{\varepsilon}{E_o} \\ \delta x' & = & 0=\delta x'_\beta+\eta'\frac{\varepsilon}{E_o} & \rightarrow \quad \delta x'_\beta=-\eta'\frac{\varepsilon}{E_o} \end{array} \tag{75}$$

Particles travel along their phase ellipses as they orbit the storage ring. The phase ellipse is described by

$$\gamma {x_\beta}^2+2\alpha x_\beta {x'}_\beta+\beta\, x'^2_\beta = a^2 \tag{76}$$

and its perturbation due to the emission of a photon is

$$\gamma\delta({x_\beta}^2)+2\alpha\,\delta(x_\beta\, x'_\beta)+\beta\,\delta(x'^2_\beta) = \delta a^2 \tag{77}$$

Replacing these variations by the results of 75 we get:

$$\begin{array}{rcl} \delta(x^2_\beta) & = & (x_{o,\beta}+\delta x_\beta)^2-x^2_{o,\beta}=2x_{o,\beta}\,\delta x_\beta+\delta x^2_\beta \\ \delta(x_\beta x'_\beta) & = & (x_{o,\beta}+\delta x_\beta)(x'_{o,\beta}+\delta x'_\beta)-x_{o,\beta}\,x'_{o,\beta} \\ & = & x_{o,\beta}\delta x'_\beta+x'_{o,\beta}\,\delta x_\beta+\delta x_\beta\,\delta {x'}_\beta \\ \delta(x'^2_\beta) & = & ({x'}_{o,\beta}+\delta {x'}_\beta)^2-x'^2_{o,\beta}=2x'_{o,\beta}\,\delta x'_\beta+\delta x'^2_\beta \end{array} \tag{78}$$

Emission of a photon can happen at any phase of the betatron oscillation and we therefore average over all phases which make the terms linear in x_β and x'_β vanish. Replacing the variations in (77) by their expressions from (79) we get

$$\delta a^2 = \frac{\langle\varepsilon^2\rangle}{E^2_o}\mathcal{H}(s) \tag{79}$$

where

$$\mathcal{H}(s) = \gamma\eta^2 + 2\alpha\eta\eta' + \beta\,\eta'^{\,2} \tag{80}$$

where we have also averaged over all photon energies. This equation looks very similar to (67) and we get the rate of change for the amplitude of the betatron oscillations analogous to (68)

$$\left\langle \frac{\mathrm{d}\langle a^2\rangle}{\mathrm{d}t} \right\rangle_{s,\text{excitation}} = \frac{\langle \dot{N}_{\mathrm{ph}}\langle\varepsilon^2\rangle\,\mathcal{H}\rangle_s}{E_o^2} \tag{81}$$

This excitation is again to be compared with damping to get an equilibrium beam emittance

$$\langle a^2\rangle_s = \tfrac{1}{2}\langle \dot{N}_{\mathrm{ph}}\langle\varepsilon^2\rangle\mathcal{H}(s)\rangle_s \tag{82}$$

The rms beam size is $\sigma_x^2 = \frac{1}{2}\langle x^2\rangle = \frac{1}{2}a^2\beta_x$ and the equilibrium beam emittance

$$\epsilon_x = \frac{\sigma_x^2}{\beta_x} = C_q\,\gamma^2\frac{\langle\mathcal{H}(s)/\rho^3\rangle}{\langle 1/\rho^2\rangle}\,. \tag{83}$$

The equilibrium beam emittance is proportional to the square of the particle energy and further depends on the strength of the bending magnets and the function $\mathcal{H}$ which is defined by the storage ring lattice. Variations in the lattice design is used to optimize a ring design for either large beam emittance (desired in colliding beam storage ring for high energy physics; many such rings were and are in use now for the production of synchrotron radiation; such storage rings are known as *first generation radiation sources*) or for very small beam emittance which can generate highest brightness synchrotron radiation beams. *Second generation* storage rings have intermediate beam emittances while *third generation* storage rings have been designed for minimum beam emittance as technically feasible at the time of design and many magnet free sections to install insertion devices.

4.5.4 Vertical Beam Emittance

We have no dispersion in the vertical plane $\eta_y \equiv 0$ and get therefore with $\mathcal{H}_y(s) = 0$ a vanishing vertical beam emittance $\epsilon_y = 0$. At this point we must acknowledge the approximation made so far. We did not consider the transverse recoil a particle may receive if a photon is emitted not exactly in the forward direction but at a finite angle within $\pm 1/\gamma$. Due to this effect $\Delta p_\perp \neq 0$ and the vertical equilibrium beam emittance turns out to be

$$\epsilon_y = \frac{\sigma_y^2}{\beta_y} = C_q\gamma^2\frac{\langle\beta_y\rangle\langle 1/\rho^3\rangle}{2\langle 1/\rho^2\rangle} \approx 10^{-13}\,\mathrm{radm} \tag{84}$$

indeed a very small emittance. This small value justifies the fact that we neglected this effect for the horizontal beam emittance. The smallest beam emittance achieved so far in any electron storage ring operated in the world is of the order of 10^{-9} rad m.

This result is actually so small that still other effects must be considered. Coupling of horizontal betatron oscillations into the vertical plane due to magnet misalignments (rotational errors of quadrupole alignment) contribute much more to the vertical beam emittance. Actually, this coupling dominates in existing storage rings the vertical beam emittance. For a well aligned storage ring ϵ_y is less than 1% of $1\epsilon_x$.

4.5.5 Photon Source Parameters

Given the betatron functions, the beam emittances and beam energy spread we define the particle beam cross section. the total beam width or height is defined by the contribution of the betatron phase space $\sigma_{\beta,x,y}$ and the energy phase space $\sigma_{\eta,x,y}$ and is

$$\sigma_{\mathrm{tot},x,y} \;=\; \sqrt{\sigma^2_{\beta,x,y} + \sigma^2_\eta} \;=\; \sqrt{\epsilon_{x,y}\beta, x, y + \eta_x^2 \frac{\sigma_\varepsilon}{E_o}} \tag{85}$$

with $\sigma^2_{\beta,x,y} = \epsilon_{x,y}\beta_{x,y}$ and $\sigma_{\eta,x} = \eta_x \frac{\sigma_\varepsilon}{E_o}$, $\gamma_{x,y} = \frac{1+\alpha^2_{x,y}}{\beta_{x,y}}$ and $\alpha_{x,y} = -\beta'_{x,y}$. Similarly, we get for the beam divergence

$$\sigma_{\mathrm{tot},x',y'} \;=\; \sqrt{\sigma^2_{\beta,x',y'} + \sigma^2_{\eta'}} \;=\; \sqrt{\epsilon_{x,y}\gamma_{x,y} + \eta'^2 \frac{\sigma_\varepsilon}{E_o}}\,. \tag{86}$$

These beam parameters resemble in general the source parameters of the photon beam. deviations occur when the beam emittance becomes very small of the order of the photon wavelength of interest. In this case the photon source parameters is are modified by diffraction effects which limit the apparent source size and divergence to some minimum values even if the electron beam cross section should be zero. For radiation at a wavelength λ the diffraction limited, radial photon source parameters are

$$\sigma_r = \frac{\sqrt{\lambda L}}{2\pi} \qquad \text{and} \qquad \sigma'_r = \sqrt{\frac{\lambda}{L}} \tag{87}$$

The projection onto the horizontal or vertical plane gives $\sigma_{x,y} = \sigma_r/\sqrt{2}$ etc. Due to diffraction it is not useful to push the electron beam emittance to values much smaller than

$$\epsilon_{x,y} \;=\; \frac{\lambda}{4\pi} \tag{88}$$

For an arbitrary electron beam cross section the photon source parameters are the quadratic sum of both contributions

$$\begin{array}{rcl} \sigma^2_{\mathrm{ph},x,y} & = & \sigma^2_{\mathrm{tot},x,y} + \frac{1}{2}\,\sigma^2_r \\ {\sigma'}^2_{\mathrm{ph},x,y} & = & {\sigma'}^2_{\mathrm{tot},x,y} + \frac{1}{2}\,{\sigma'}^2_r \end{array} \tag{89}$$

5 Storage Ring Design Optimization

Synchrotron radiation sources have undergone significant transitions and modifications over the past 30 or so years. Originally, most experiments with synchrotron radiation were performed parasitically on high energy physics colliding beam storage rings. Much larger photon fluxes could be obtained from such sources than from any other source available then. The community of synchrotron radiation users grew rapidly and so did the variety of applications and fields. By the time the usefulness of storage rings for high energy physics was exhausted some of these facilities were turned over to the synchrotron radiation community as fully dedicated radiation sources. Those are called now the *first generation* synchrotron radiation sources. They were not optimized for minimum beam emittance and maximum photon beam brightness. Actually, the optimization for high energy physics called for a maximum beam emittance to maximize collision rates for elementary particle events. The radiation sources were mostly bending magnets although the development and use of insertion devices started in these rings.

As the synchrotron radiation community further grew, funds became available to construct dedicated radiation facilities. Generally these rings were designed as bending magnet sources but with reduced beam emittance to increase photon brightness. The design emittances were much smaller than those of first generation rings but still large by present day standards. The use of insertion devices did not significantly affect the storage ring designs yet. These rings are called *second generation* rings.

Third generation synchrotron radiation sources have been designed and constructed during the second half of the eighties and into the nineties. These rings were specifically designed for insertion device radiation and minimum beam emittance or maximum photon beam brightness. As such they exhibit a large number of magnetfree insertion straight sections.

Finally, *fourth generation* synchrotron radiation sources are so far only under discussion. A consensus seems to emerge within the community that such sources may be based more on linear accelerators than on storage rings. For example, great efforts are underway in a number of laboratories to design a x-ray lasers. Such a source would be based on the principle of a single pass FEL where a high energy and quality electron beam passing through a long undulator produces undulator radiation in the x-ray regime.

5.1 Storage Ring Lattices

To achieve a small particle beam emittance for maximum photon beam brightness a number of different magnet lattices for storage rings are available. All lattices can basically be used to achieve as small a beam emittance as desired, limited only by diffraction effects of the photon beams. Other more practical considerations, however, will limit the minimum beam emittance achievable in any lattice. A variety of magnet lattices have been used and proposed in existing storage rings synchrotron radiation sources under construction. In this section three basic types and some variations thereof will be discussed:

- the FODO lattice
- the double bend achromat lattice (dba)
- the triple bend achromat lattice (tba)

All lattice types can provide long magnet free sections for the installation of insertion devices, accelerating cavities and injection components. For insertion devices one would prefer to have dispersion free sections available which is easy to achieve in a dba- or tba-lattice but somewhat complicated in a FODO lattice. On the other hand a FODO lattice is very compact and is therefore mostly suitable for generating low emittance beams in so-called damping rings for applications in high energy accelerator systems. The dba- and tba-lattice is more open and providing easily magnetfree straight sections, a feature mostly desired for high brightness synchrotron radiation sources. We consider here briefly the FODO lattice because of its simplicity and its ability to give us a quick feeling for the scaling of beam emittance with lattice parameters.

5.1.1 FODO Lattice

What is $\mathcal{H}(s) = \gamma\eta^2 + 2\alpha\eta\eta' + \beta\,\eta'^{\,2}$ in a FODO lattice ? To calculate the average value of $\mathcal{H}$ in a FODO lattice is somewhat elaborate. Here, we are interested primarily in the scaling of the beam emittance with FODO lattice parameters. Recollecting the results for the symmetric solutions of the lattice functions in a FODO lattice, Eqs. (45) and (47) we notice the following scaling laws

$$\beta \propto L \qquad\qquad \beta' \propto L^0 \tag{90}$$

$$\eta \propto L^2/\rho \qquad\qquad \eta' \propto L/\rho \tag{91}$$

With this we find that all three terms in the function $\mathcal{H}(s)$ scale like

$$\{\mathcal{H}(s)\} = \left\{\frac{1}{L}\frac{L^4}{\rho};\, L^0\frac{L^2}{\rho}\frac{L}{\rho};\, L\frac{L^2}{\rho}\right\} \propto \frac{L^3}{\rho^2} \tag{92}$$

and the equilibrium emittance for a FODO lattice scales than like

$$\epsilon_x = C_q\gamma^2\frac{\langle\mathcal{H}/\rho\rangle}{\langle 1/\rho^2\rangle} \propto \gamma^2\frac{L^3}{\rho^3} \propto \gamma^2\varphi^3 \tag{93}$$

where $\varphi = \ell_\mathrm{b}/\rho$ is the deflection angle in each bending magnet. The proportionality factor depends on the strengths of the quadrupoles and is large for very weak or very strong quadrupoles. A minimum can be reached for a focal length of $|f| \approx 1.06L$ in each half-quadrupole resulting in a minimum beam emittance achievable in a FODO lattice given in practical units by

$$\epsilon\,(\mathrm{radm}) \approx 10^{-11}\,E^2(\mathrm{GeV})\,\varphi^3\,(\mathrm{deg}^3)\,, \tag{94}$$

where $\varphi = 2\pi/N_M$, N_M the number of bending magnets in the ring and $N_M/2$ the total number of FODO cells in the ring. This result is significant because it exhibits a general scaling of the beam emittance in all lattices proportional to the square of the beam energy and the cube of the deflecting angle in each bending magnet. While the beam energy is primarily driven by the desired photon spectrum we find that high brightness photon beams from low emittance electron beams require a storage ring design involving many lattice cells with a small deflection angle per magnet. Of course, there are some limits on how far one can go with this concept due to some other limitations, one being size and cost of the ring which both grow with the number of lattice cells.

5.2 Optimization of a Storage Ring Lattice

While the cube dependence of the beam emittance on the bending angle is a significant design criterion we discuss here a more detailed optimization strategy. The emittance is determined by the beam energy, the bending radius and the $\mathcal{H}$- function. Generally, we have no choice on the beam energy which is mostly determined by the desired critical photon energy of bending magnet and insertion device radiation or cost. Similarly, the bending radius is defined by the ring geometry, desired spectrum etc. Interestingly, we will see that it is not the bending radius but rather the bending angle which influences the equilibrium beam emittance. The main process to minimize the beam emittance is to adjust the focusing such that the lattice functions in the bending magnets generate a minimum value for $\langle\mathcal{H}\rangle$.

5.2.1 Minimum Beam Emittance

The equilibrium beam emittance (83)

$$\epsilon_x = \frac{\sigma_x^2}{\beta_x} = C_q\,\gamma^2\,\frac{\langle\mathcal{H}(s)/\rho^3\rangle}{\langle 1/\rho^2\rangle} \tag{95}$$

depends only on the lattice function $\mathcal{H}(s)$ inside bending magnets where $1/\rho \neq 0$. We may therefore, independent of any lattice type, consider this function only within bending magnets and look for minimization procedures. In a regular periodic lattice it can be assumed that all lattice functions within one bending magnet are the same as in all others and we may concentrate therefore our discussion just on one bending magnet. The average value $\langle\mathcal{H}/\rho^3\rangle$ for the whole ring will then be the same as that for one magnet.

The contribution of any individual bending magnet with bending radius ρ to the beam emittance can be determined by calculation of the average:

$$\langle\mathcal{H}\rangle = \frac{1}{\ell_\mathrm{b}}\int_o^{\ell_\mathrm{b}} \mathcal{H}(s)\,\mathrm{d}\,s \tag{96}$$

where L is the length of the bending magnet and the bending radius is assumed to be constant within a magnet. From here on we ignore the index x since

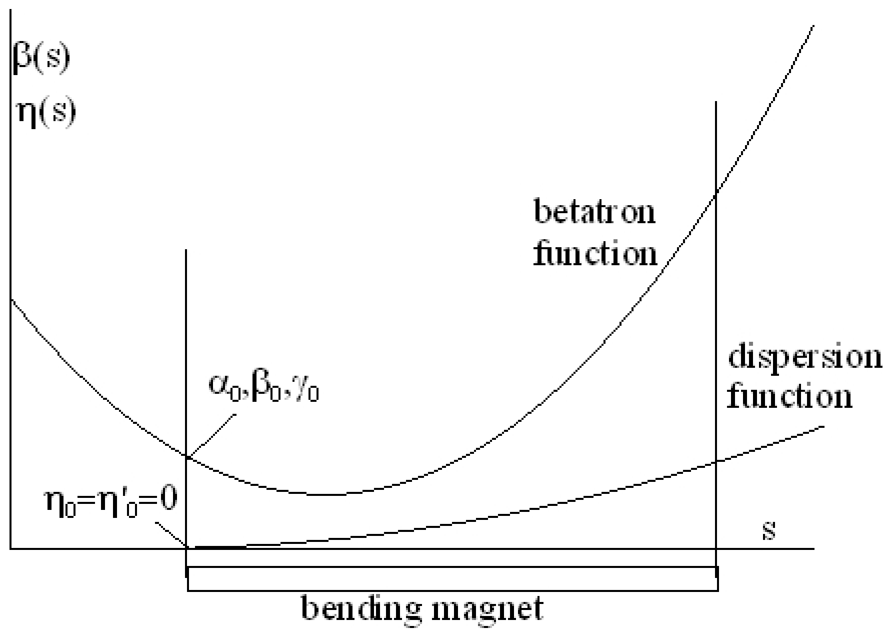

Figure 12: Betatron Functions within a Bending Magnet

we assume a flat storage ring in the horizontal plane. All lattice functions are therefore to be taken in the horizontal plane. Since in first approximation there is no focusing within bending magnets we may treat such magnets as drift spaces. We may express the lattice functions within the bending magnet starting with $\beta_o, \alpha_o, \gamma_o$ at the beginning of the magnet by (Fig. 12)

$$\begin{aligned}
\beta(s) &= \beta_o - 2\alpha_o s + \gamma_o s^2 \\
\alpha(s) &= \alpha_o - \gamma_o s \\
\gamma(s) &= \gamma_o \\
\eta(s) &= \eta_o + \eta_o' s + \rho(1 - \cos\psi) \\
\eta'(s) &= \eta_o' + \sin\psi
\end{aligned} \tag{97}$$

where s varies between zero and ℓ_b and the deflection angle $\psi = \frac{s}{\rho}$. Before we use these equations we assume lattices where $\eta_o = \eta_o' = 0$. The consequences of this assumption will be discussed later. Using (96) and (98) we get :

$$\langle \mathcal{H} \rangle = \beta_o B + \alpha_o \rho A + \gamma_o \rho^2 C \tag{98}$$

The coefficients A, B, and C are functions of the total deflection angle $\varphi = \ell_\mathrm{b}/\rho$

defined by:

$$
\begin{aligned}
B &= \frac{1}{2}\left(1 - \frac{\sin 2\varphi}{2\varphi}\right) \\
A &= 2\,\frac{1-\cos\varphi}{\varphi} - \frac{3}{2}\,\frac{\sin^2\varphi}{\varphi} - \frac{1}{2}\,\varphi + \frac{1}{2}\,\sin 2\varphi \\
C &= \frac{3}{4} + 2\cos\varphi + \frac{5}{4}\,\frac{\sin\,2\varphi}{2\varphi} - 4\,\frac{\sin\,\varphi}{\varphi} + \frac{1}{6}\,\varphi^2 \\
&\quad -\frac{1}{4}\,\varphi\sin\,2\varphi + \frac{3}{2}\,\sin^2\varphi
\end{aligned}
\tag{99}
$$

For small bending angles and an isomagnetic ring where all bending magnets are the same we have:

$$
\begin{aligned}
B &\approx \frac{1}{3}\,\varphi^2\,(1 - \frac{1}{5}\,\varphi^2\,) \\
A &\approx -\frac{1}{4}\,\varphi^3\,(1 - \frac{5}{18}\,\varphi^2\,) \\
C &\approx \frac{1}{20}\,\varphi^4\,(1 - \frac{5}{14}\,\varphi^2\,)
\end{aligned}
\tag{100}
$$

and the beam emittance in the lowest order of approximation in becomes

$$
\epsilon = C_q\,\gamma^2\,\varphi^3\;\left\{\frac{1}{3}\left(\frac{\beta_o}{\ell_{\mathrm{b}}}\right) - \frac{1}{4}\,\alpha_o + \frac{\gamma_o\,\ell_{\mathrm{b}}}{20}\right\}
\tag{101}
$$

where C_q is defined in (72).

This equation shows clearly a cubic dependence of the beam emittance on the deflection angle φ in the bending magnets, which is a general property of all lattices since we have not yet made any assumption on a particular lattice. Equation (101) has a minimum for both α_o and β_o. We calculate the derivative $\frac{\partial}{\partial \alpha_o}\,\langle\mathcal{H}\rangle = 0$ for α_o and get:

$$
\alpha_{o\,\mathrm{opt}} = -\frac{1}{2}\,\frac{A}{C}\,\frac{\beta_o}{\rho}
\tag{102}
$$

Inserting this result into (101), evaluating the derivative $\frac{\partial}{\partial\,\beta_o}\,\langle\mathcal{H}\rangle = 0$ and solving for β_o we get:

$$
\beta_{o\,\mathrm{opt}} = \frac{2\,C\,\rho}{\sqrt{4BC - A^2}}
\tag{103}
$$

With $\beta_{o\,\mathrm{opt}}$ we express $\alpha_{o\,\mathrm{opt}}$ by :

$$
\alpha_{o\,\mathrm{opt}} = \frac{-A}{\sqrt{4BC - A^2}}
\tag{104}
$$

and get finally the minimum possible value for $\mathcal{H}$:

$$
\langle\mathcal{H}\rangle_{\mathrm{min}} = \sqrt{4BC - A^2}\,\rho
\tag{105}
$$

For small deflection angles $\varphi \ll 1$ the optimum lattice functions at the entrance to the bending magnets are with $\eta_0 = \eta_0' = 0$:

$$\begin{aligned}
\alpha_{0\,\mathrm{opt}} &\approx \frac{(1-\frac{5}{18}\,\varphi^2\,)\sqrt{15}}{\sqrt{1-\frac{61}{105}\varphi^2}} \approx \sqrt{15}\left(1+\frac{4\varphi^2}{315}\right) \\
&\approx \sqrt{15}, \qquad (106) \\
\beta_{0\,\mathrm{opt}} &\approx \frac{\sqrt{12}\,(1-\frac{5}{14}\,\varphi^2)\,\ell_\mathrm{b}}{\sqrt{5}\,\sqrt{1-\frac{61}{105}\,\varphi^2}} \approx \sqrt{\frac{12}{5}}\,\ell_\mathrm{b}\left(1-\frac{7\varphi^2}{105}\right) \\
&\approx \sqrt{\frac{12}{5}}\,\ell_\mathrm{b}, \qquad (107) \\
\langle\mathcal{H}\rangle_\mathrm{min} &\approx \frac{\varphi^3\,\rho}{4\,\sqrt{15}}\sqrt{1-\frac{61}{105}\,\varphi^2} \approx \frac{\varphi^3\,\rho}{4\,\sqrt{15}}\left(1-\frac{61\varphi^2}{210}\right) \\
&\approx \frac{\varphi^3\,\rho}{4\,\sqrt{15}}. \qquad (108)
\end{aligned}$$

With this the minimum obtainable beam emittance in any lattice with the assumed bending magnet parameters is from (83)

$$\epsilon_\mathrm{dba,min} = C_q\,\gamma^2\,\frac{\langle\mathcal{H}(s)/\rho^3\rangle}{\langle 1/\rho^2\rangle} = C_q\,\gamma^2\,\frac{\varphi^3}{4\sqrt{15}} \qquad (109)$$

The results are very simple for small deflection angles but for angles larger than about 33° per bending magnet the error for $\langle\mathcal{H}\rangle_\mathrm{min}$ exceeds 10%. For smaller storage rings with few bending magnets higher order terms in φ must be taken into account. It is interesting to note that the next order correction due to larger bending angles gives a reduction beam emittance compared to the lowest order approximation. Higher order terms, however, quickly stop and reverse this reduction

For simplicity we assumed that the dispersion functions $\eta_o = 0$ and $\eta_o' = 0$. Numerical methods must be used to find the optimum solutions for finite dispersion functions. In the following we consider only very small values $\eta_o \ll 1$ and $\eta_o' \ll 1$ to evaluate the impact of the correction for a finite dispersion on the beam emittance. Retaining only linear terms in η_o, η_o', φ the $\langle\mathcal{H}\rangle$ is:

$$\langle\mathcal{H}\rangle_{\eta\,\mathrm{min}} = \langle\mathcal{H}\rangle_\mathrm{min} + \frac{1}{\sqrt{5}}\left(\frac{5}{3}\,\eta_o + 6\,\eta_o'\,\ell_\mathrm{b}\right)\varphi \qquad (110)$$

Obviously a further reduction in the beam emittance can be obtained for negative values of η_o and η_o'. This has been exploited in recent storage ring designs. Nonlinear terms, however, cause quickly an increase in the beam emittance again and the gain seems minimal.

In summary it has been demonstrated that there are certain optimum conditions for lattice functions in bending magnets to minimize the equilibrium beam emittance. No assumption about a particular lattice has been made yet.

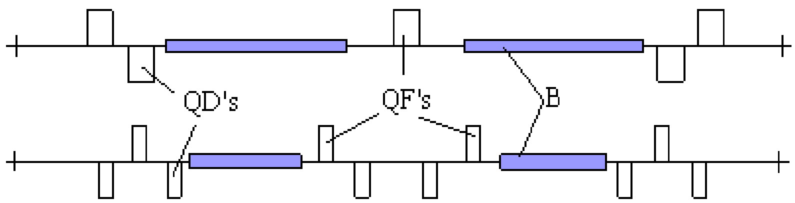

Figure 13: dba-Lattice,schematic

Another observation is that the beam emittance is proportional to the third power of the magnet deflection angle suggesting to design for small deflection angles in order to achieve a small beam emittance. Low emittance storage rings therefore are characterized by many short magnet lattice periods.

5.2.2 The Double Bend Achromat (dba) Lattice

The dba-lattice is designed such as to make full use of the minimization possibilities for the beam emittance as just discussed and to provide dispersionfree insertion straight sections. Fig. 13 shows two renditions of the basic layout for a dba-lattice. Other slightly different modifications have been used but the basic design features are the same. Starting from the middle of an insertion straight section a set of two or more quadrupoles provide the proper focusing of the lattice functions into the bending magnet to achieve the minimum beam emittance. The insertions are kept dispersion free which is the main function of the focusing between the dipole magnets. The section between and including the bending magnets is called an *achromat* because the dispersion is zero outside of the achromat.

The ideal minimum beam emittance in this lattice type is from (109)

$$\epsilon_{\mathrm{dba}} \;=\; \frac{C_q}{4\sqrt{15}}\,\gamma^2\,\varphi^3 \tag{111}$$

or in more practical units:

$$\epsilon_{\mathrm{dba}}\,(\mathrm{rad\,m}) \;=\; 5.036\times 10^{-13}\,E^2(\mathrm{GeV}^2)\,\varphi^3\,(\mathrm{deg}^3) \tag{112}$$

To achieve this minimum beam emittance we must provide specific values for the lattice functions at the entrance to the bending magnets. Specifically, the initial horizontal betatron function must be strongly convergent reaching a minimum about one third through the bending magnet. At the end of the bending magnet the ideal betatron, however, becomes quite large. Note, that the vertical lattice functions can be chosen freely since they do not affect the beam emittance as long as there is no vertical bending.

In an actual lattice design it appears difficult to achieve sufficient beam stability if the lattice parameters at the entrance to the bending magnets are

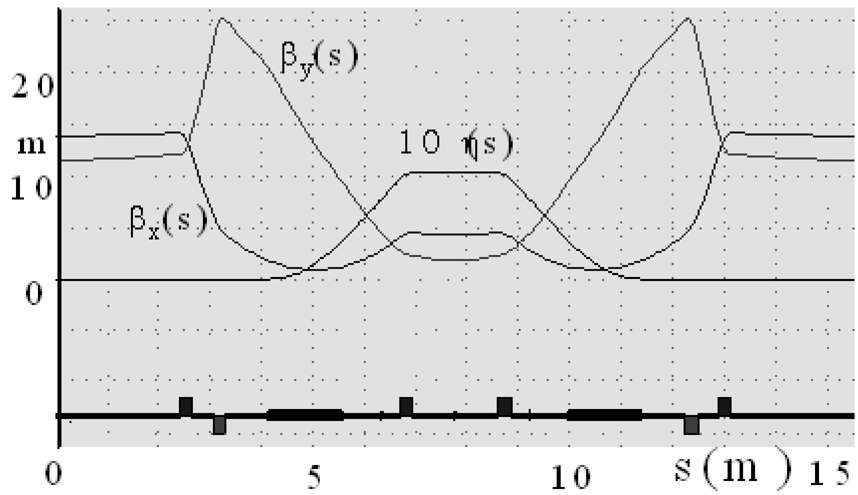

Figure 14: DBA-Lattice of Synchrotron Light Source at the LNLS, Brazil

set to the optimum values. A compromise between optimum lattice parameters and beam stability must be reached resulting in a somewhat increased beam emittance compared to the theoretical minimum. The source of the problem are the large values of the betatron function at the exit of the bending magnet causing strong chromatic aberrations which must be corrected by sextupole magnets. This correction is less than ideal and generates in turn geometric aberrations and a compromise between correction of chromatic and generating geometric aberrations must be made. The result of this compromise in a well designed storage ring must be a sufficiently large aperture within which the beam can travel for many hours without losses. Outside of this aperture, called the *dynamic aperture*, particles are lost due to geometric aberrations. Generally, a sufficiently large dynamic aperture cannot be obtained for the ideal solution of minimum beam emittance. On the other hand, the dynamic aperture grows rapidly as the optimum conditions on the lattice functions are relaxed.

An example of a working dba lattice is shown in Fig. 14 for the recently constructed 1.3 GeV storage ring at the Laboratorio National de Luz Sincrotron (LNLS) in Campinas, Brazil.

The central part of the lattice between the bending magnets may consist of one to four quadrupoles and its only function is to focus the dispersion function so that all insertions are dispersion free. This results necessarily in a betatron phase advance from bending magnet to bending magnet of close to 180°. In the insertions the betatron function is generally kept large to optimize undulator photon beam characteristics and therefore the betatron phase advance is small. As a result the tune of the ring is quite fixed and cannot be adjusted independently without also changing significantly the insertion characteristics

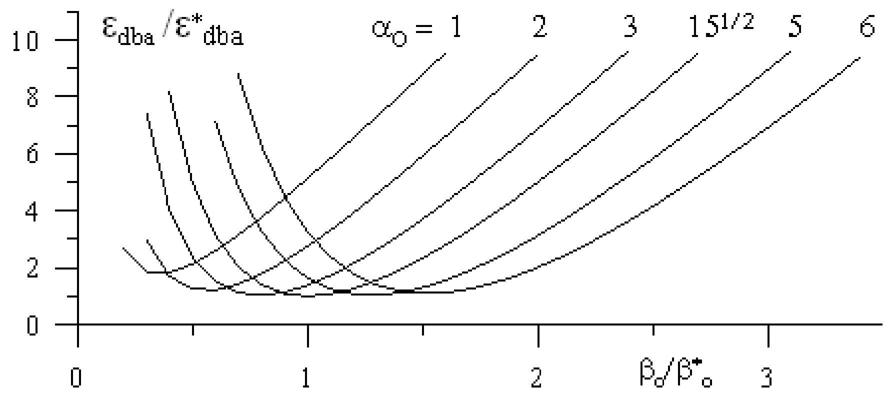

Figure 15: Emittance and lattice functions in a dba lattice

and beam emittance. These limitations quickly vanish if the storage ring is not designed for minimum beam emittance. At larger values of the beam emittance the lattice becomes more flexible.

The choice of the optimum value for $\alpha_o^* = \sqrt{15}$ causes the betatron function to reach a sharp minimum at about one third into the bending magnet, $s_{\min} = \frac{\alpha_o^*}{\gamma_o^*} = \frac{3}{8}\,\ell_{\mathrm{b}}$, and to increase from there on to large values causing problems with nonlinear aberrations. For arbitrary values of α_o, however, there is still a relative optimum value for β_o. We evaluate the derivative $\frac{\partial}{\partial\beta_o}\langle\mathcal{H}\rangle = 0$ only and solve for :

$$\frac{\beta_o}{\ell_{\mathrm{b}}} = \sqrt{\frac{3}{20}}\,\sqrt{1 + \alpha_o^2} \tag{113}$$

The beam emittance in this case can be expressed in units of the minimum beam emittance $\epsilon_{\mathrm{dba}}^*$ and we get from (30):

$$\frac{\epsilon_{\mathrm{dba}}}{\epsilon_{\mathrm{dba}}^*} = \frac{1}{2}\,\gamma_o\,\beta^* + 8\,\frac{\beta_o}{\beta^*} - \sqrt{15}\,\alpha_o \tag{114}$$

where $\gamma_o = \frac{1+\alpha_o^2}{\beta_o}$. Equation (114) is plotted in Fig. 15 for different values of α_o as a function of β/β^*.

It is apparent from Fig. 15 that the minimum emittance changes only little even for big variations of α_o about its optimum value allowing us to choose much more forgiving values for $\alpha_o$without much loss in beam emittance. This weak dependence can be used to lessen the problems caused by nonlinear aberrations. The maximum value of the betatron function $\beta(\ell_{\mathrm{b}})$ at the end of the bending magnet reaches a minimum for $\alpha_o = \frac{4\sqrt{15}}{17}$ at the expense of a loss in beam emittance of about a factor of two. For this condition

$$\frac{\alpha_o}{\alpha_o^*} = \frac{4}{17}; \quad \frac{\beta_o}{\beta_o^*} = \frac{23}{68}\,\frac{\beta(\ell_{\mathrm{b}})}{\beta_o^*(\ell_{\mathrm{b}})} = \frac{17}{32}; \quad \frac{\epsilon_{\mathrm{dba}}}{\epsilon_{\mathrm{dba}}^*} = \frac{32}{17} \tag{115}$$

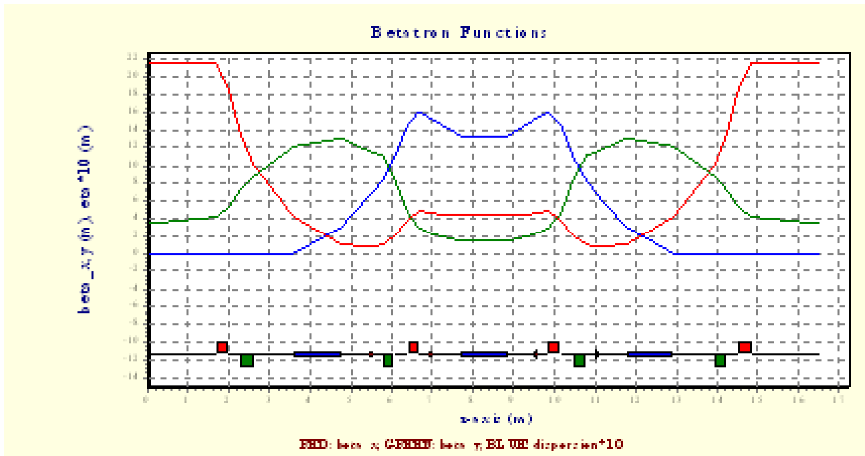

Figure 16: Implementation of a triple bend achromat lattice at the National Synchrotron Radiation laboratory, NSRL in Hefei, China

5.2.3 The Triple Bend Achromat (tba) Lattice

As a variation of the dba lattice a *triple bend achromat* lattice has become popular in recent synchrotron radiation source designs. In this case three bending magnets are placed between each pair of insertion straight sections (Fig.16). That results in a reduction of the circumference by about 33% although at the expense of a similar reduction in available insertion straight sections. This lattice type serves well for smaller facilities and lower energies.

5.3 Limiting Effects

Given the usefulness of maximum photon beam brightness for experimenters one might wonder why don't we just design storage rings with a beam emittance below the diffraction limit. The answer has to do with limitations of beam stability due to nonlinear betatron oscillations. To reduce the beam emittance we require stronger and/or more quadrupole focusing. The energy spread in the beam causes a variation of focusing with lower energy particles being focused to much and higher energy particles focused too little. The total amount of focusing in a storage ring is a measure for these *chromatic aberrations*. Such aberrations can cause a spread in the tunes due to the finite energy spread in the beam and one might hit a resonance. Chromatic aberrations can also cause a direct beam instability. For those reasons we must compensate the chromatic aberrations which we call the *chromaticity* in storage ring physics. There are two chromaticities, one for the horizontal and the other for the vertical plane.

Correction of the chromaticities can be accomplished by installing sextupoles into the storage ring at locations where the dispersion is not zero. the dispersion

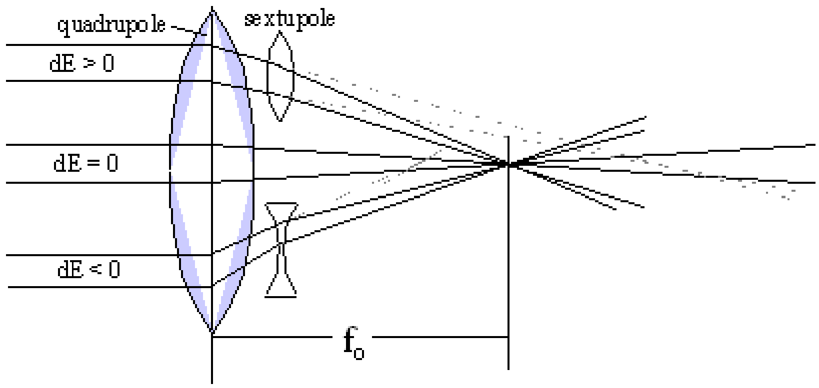

Figure 17: Correction of Chromatic Aberrations

causes some degree of segregation between the higher and lower energy particles with the higher energy particles gathering more outside of the ideal orbit and the lower energy particles more on the inside. Sextupoles can be considered as quadrupoles with varying focal strength across the horizontal aperture. A sextupole therefore can add some focusing for higher energy particles being outside of the ideal orbit ($x > 0$) and subtract some focussing for lower energy particles at $x < 0$ (Fig. 17). That compensated the under and over focusing these particles experienced in the regular quadrupoles. Distributing sextupoles around the ring is the therefore the preferred way to compensate the storage ring chromaticity.

Every coin has two sides, however. The sextupole field increases quadratically with x and while we compensate the chromaticities these same sextupoles generate nonlinear, quadratic perturbations especially for particles with large betatron oscillation amplitudes. These perturbations are known as *geometric aberrations* generating pillowcase perturbations in the images well known from light optics. The art of storage ring design is then to correct the chromatic aberrations while keeping the geometric aberrations at a minimum. This can be achieved up to a certain degree by distributing sextupoles along the orbit at properly selected locations. Yet, since we deal with a nonlinear problem we cannot expect to get a perfect compensation. There will always be a limit on the maximum stable betatron oscillation amplitude in the storage ring. The design objective is then to expand the limit for large amplitude betatron oscillations. This limit is called the *dynamic aperture* in contrast to the physical aperture defined by the vacuum chamber. There is no analytical solution for the dynamic aperture and it is determined by numerical particle tracking programs which follow individual particles for some thousand turns through all nonlinear fields.

For a stable beam with a long beam lifetime we must have a minimum dynamic aperture to accommodate not only the beam proper but also a halo of particles around the beam. This halo is made-up of particles which have been deflected by a small angle during the elastic collision with a residual gas atom. Such collisions occur quite frequently, constantly populating the halo with new particles. By damping these particles loose betatron oscillation amplitudes and leave slowly the halo again to join the beam proper. While there are only few particles in the halo at any one time we cannot scrape off this halo by lack of sufficient dynamic aperture. the beam lifetime would be reduced quickly since there is a constant flow of particles into the halo and back to the beam. This flow cannot be interrupted.

As we increase the focusing in an attempt to minimize the beam emittance we also must increase the amount of chromaticity correction in from of sextupole fields. This, however, also increases the total geometric aberrations and as a consequence we find a reduced and unacceptable dynamic aperture. Further studies and understanding of nonlinear dynamics in storage rings is required to hopefully improve our skill for chromaticity corrections and thereby reduce the minimum achievable beam emittances.